RC 1401

Investigation of Transverse Cracking On Michigan PCC Pavements over Open-Graded Drainage Course

Final Report

To

Michigan Department of Transportation

Department of Civil and Environmental Engineering

The University of Michigan
College of Engineering

Ann Arbor, MI 48109-2125

TESTING AND RESEARCH SECTION
CONSTRUCTION AND TECHNOLOGY DIVISION
RESEARCH PROJECT - RC-1401

Investigation of Transverse Cracking On Michigan PCC Pavements over Open-Graded Drainage Course

Final Report

To

Michigan Department of Transportation

By

Will Hansen,
Andrew Definis, Elin Jensen, Christopher R. Byrum,
Ashraf R. Mohamed, Phil Mohr, Gail Grove

Department of Civil and Environmental Engineering
University of Michigan

And
Thomas J. Van Dam,
Matthew Wachholz
Department of Civil Engineering
Michigan Technological University

November 30, 1998

Technical Report Documentation Page

1. Report No.	2. Government Accession No.	3. Recipient's Catalog No.

4. Title and Subtitle	5. Report Date
Investigation of Transverse Cracking On Michigan PCC Pavements over Open-Graded Drainage Course	November 30, 1998
	6. Performing Organization Code
	8. Performing Organization Report No.
7. Author(s) Will Hansen, Elin Jensen, Andrew Definis, UM	
9. Performing Organization Name and Address University of Michigan, Dept. of Civil & Environmental Engineering 2340 G. G. Brown, 2350 Hayward Ann Arbor, MI 48109-2125	10. Work Unit No. (TRAIS)
	11. Contract or Grant No.
	13. Type of Report and Period Covered
12. Sponsoring Agency Name and Address	
	14. Sponsoring Agency Code

15. Supplementary Notes

16. Abstract

Some OGDC projects have developed premature transverse cracking with associated spalling and faulting. The objective of this project was to investigate these projects to determine the cause(s) of the cracking and the relationships, if any, the cracking may have with the OGDC base layer.

Field measurements were used to quantify the amounts of transverse cracking and spalling for each project. The results were plotted versus pavement age. In general, both distress types follow expected trends over time with very little, if any, spalling development during the first 10 years. These results corroborate MDOT findings using PMS performance data that indicates there is no premature deterioration of OGDC pavements compared to pavements constructed on dense-graded bases. However some pavements (CS 77023, 77024A) have developed severe spalling and faulting after 13 years. The most plausible reasons for the associated distress were trapped water in the subbase/subgrade and clogged outlet drains. No evidence was found that indicates the OGDC by itself was a major contributor to the observed severe distress.

The occurrence of premature transverse cracking on I-94 EB near Watervliet, CSN 11017, within the first few years after construction is believed to have resulted from the interaction of several factors, all associated with hot weather construction. Based on a review of MDOT construction records, it appears that mid-slab transverse cracking is associated with several related factors: (1) high slab placement temperatures approaching 90 °F, (2) adverse environmental conditions (sunny and hot daytime temperatures and cool nights) which lead to significant thermal stresses, and (3) late saw cutting of joints. Mid-depth (5-6 inches) edge cracking had developed originating at the slab surface within a year and a half from construction. A field visit and coring conducted six months later found that some of these cracks had propagated into full-width, full-depth cracks. Traffic loadings likely helped the crack to propagate.

Low load transfer efficiency (LTE) values at cracks and joints were measured with the FWD on the EB I-94 JPCP project. LTE values of 35% were typical for the approach joint/crack, and 70% for the leave joint/crack for this project. These large differences in LTE values on either side of a joint or crack were found only with concrete pavement containing slag as coarse aggregate. One plausible reason is that faulting begins on the approach side of a crack or joint. Perhaps a 3G OGDC gradation, which does not follow a 0.45 power curve closely, may not provide sufficient stability to heavy loading at joints and cracks for slag PCC.

The results from this study suggest that improvements in both construction and in the concrete mix are needed. Given that MDOT is moving towards JPCP as it's standard pavement type, premature mid-slab cracking and spalling must be avoided. High PCC placement temperatures (>80 °F), especially during morning hours on hot summer days, should be avoided as premature transverse cracking can be expected. Nighttime paving would help reduce this problem.

17. Key Words	18. Distribution Statement
Open-Graded Drainage Course, Pavement Performance, PCC pavements, Spalling and Faulting, Transverse Cracking	

19. Security Classif. (of this report)	20. Security Classif. (of this page)	21. No. of Pages	22. Price

Form DOT F 1700.7 (8-72) Reproduction of completed page authorized

Acknowledgments

The research described in this project was sponsored by the Michigan Department of Transportation (MDOT) under the Pavement Research Center of Excellence (PRCE) program. The authors gratefully acknowledge the financial support, and wish to extend their sincere appreciation and thanks to John Staton, MDOT Technical Advisory Group (TAG) chairman and to David Smiley, MDOT, for their support and cooperation, and for their guidance throughout this study.

This project could not have been carried out without the cooperation and help of many of the officials at the Michigan Department of Transportation (MDOT). A special thanks to: Kurt Bancroft for conducting the FWD testing and for providing traffic control. Often times his workday started before dawn and commenced late afternoons. Without his helpfulness and flexibility in scheduling field work this study could not have been executed as smoothly as it was.

Thanks to Bob Kelly for coring, Connie Houk, Dawn Langlois and Dennis Dodson for providing the research team with the Pavement Management System (PMS) data.

Thanks is also extended to Mike Green and Jerry Sweeney for providing the research team with valuable project information.

The authors also wish to thank Dr. Starr Kohn of the Soil and Materials Engineers, Inc. (SME), Plymouth, Michigan for loaning a Dynamic Cone Penetrometer (DCP) to the research team.

Disclaimer

This document was prepared and is being disseminated under the sponsorship of the Michigan Department of Transportation. The sponsoring agency assumes no liability for its contents or use thereof. The contents of this report reflect the views of the contractor, who is responsible for the accuracy of the data presented herein. This report does not constitute a standard, specification or regulation.

The Michigan Department of Transportation does not endorse products or manufacturers. Trade or manufacturers names appear herein only because they are considered essential to the object of this document.

TABLE OF CONTENTS

Appendices

A. OGDC Sections in Michigan
B. Section Summaries and Control Section Logs
C. Pavement Distress
D. Selected Site Photos
E. Construction Records
F. Pavement Management System Data
G. Concrete Properties
H. Foundation Properties
I. Dynamic Cone Penetrometer (DCP) Data
J. Falling Weight Deflectometer (FWD) Data
K. Resilient Modulus Data, Study of Resilient Modulus and ASSHTO Serviceability for OGDC Materials
L. Literature Review

Executive Summary

In 1984, the Michigan Department of Transportation (MDOT) adopted open-graded drainage course (OGDC) as the standard base layer directly below portland cement concrete (PCC) pavements. At that time, jointed reinforced concrete pavement (JRCP) with a 41 ft. slab length was Michigan's standard design. Since initiation, the gradation of the OGDC base has varied. Approximately 45 projects, totaling 650 lane miles, have been constructed with OGDC bases. MDOT has used various OGDC gradations to find the optimal mix that achieves both a stable and drainable layer.

Some OGDC projects have developed premature transverse cracking with associated spalling and faulting. The objective of this project was to investigate these projects to determine the cause(s) of the cracking and the relationships, if any, the cracking may have with the OGDC base layer.

The initial scope of the project included a detailed field and laboratory investigation of six OGDC projects and three comparison projects with a dense-graded base course (DGBC), which were constructed in the mid-1980's. Except for one DGBC project on I-475 in Flint, all the projects are located on I-69 between Lansing and Port Huron. In the second year of the study, a jointed plain concrete pavement (JPCP) project on I-94, near Watervliet, was added. EB I-94, which has mid-slab transverse cracking, was constructed in September 1995, while WB I-94 with no apparent cracking was constructed the following spring in 1996.

Field measurements were used to quantify the amounts of transverse cracking and spalling for each project. The results were plotted versus pavement age. In general, both distress types follow expected trends over time with very little, if any, spalling development during the first 10 years. These results corroborate MDOT findings using PMS performance data that indicates there is no premature deterioration of OGDC pavements compared to pavements constructed on dense-graded bases. However some pavements (CS 77023, 77024A) have developed severe spalling and faulting after 13 years. The most plausible reasons for the associated distress were trapped water in the subbase/subgrade and clogged outlet drains. No evidence was found that indicates the OGDC by itself was a major contributor to the observed severe distress.

For OGDC pavements, the literature suggests that enhanced pavement performance will result if the drainage system is maintained. This is consistent with the findings of this study, which found that pavement sections suffering high amounts of distress, such as 77024A and 77023, also had evidence of poor drainage, whereas pavements with good performance, such as 19042B and 19042C, had operating drainage systems.

The occurrence of premature transverse cracking on I-94, EB, near Watervliet, CSN 11017, within the first few years after construction is believed to have resulted from the interaction of several factors, all associated with hot weather construction. Based on a review of MDOT

construction records it appears that mid-slab transverse cracking is associated with several related factors: (1) high slab placement temperatures approaching 90 °F, (2) adverse environmental conditions (sunny and hot daytime temperatures and cool nights), which lead to significant thermal stresses, and (3) late saw cutting of joints. These conditions were present for the JPCP project on I-94 near Watervliet, where mid-depth (5-6 inches) edge cracking had developed originating at the slab surface within a year and a half from construction. A field visit and coring conducted six months later found that some of these cracks had propagated into full-width, full-depth cracks. Traffic loadings likely helped the crack to propagate.

Low load transfer efficiency (LTE) values at cracks and joints were measured with the FWD on the EB I-94 JPCP project. LTE values of 35% were typical for the approach joint/crack, and 70% for the leave joint/crack for this project. These large differences in LTE values on either side of a joint or crack were found only with concrete pavement containing slag as coarse aggregate. One plausible reason is that faulting begins on the approach side of a crack or joint. Perhaps a 3G OGDC gradation, which does not follow a 0.45 power curve closely, may not provide sufficient stability to heavy loading at joints and cracks for slag PCC.

The PCC field strength was investigated to determine if the mechanical properties such as compressive strength, tensile strength from split cylinder tests, and elastic modulus, were deficient. In all cases it was found that the field compressive strength of all the investigated sections substantially exceeded the 28-day minimum strength requirement of 3,500 psi. The average field compressive strength for the older sections (i.e. without the I-94 JPCP project) was 6,619 psi with a low of 5,670 psi (CSN 25132) and a high of 7,450 psi (CSN 44044). Overall the mechanical properties did not vary significantly between the different projects and thus cannot explain the observed differences in pavement performance.

For the JRCP's investigated for this study, FWD analysis shows that crack widths greater than about 25 mils (0.6mm) have rapidly decreasing LTE's and higher frequency of spalling. These results suggest that spalling of cracks may be associated with the increased deflection from heavy traffic loading. This finding may be useful to MDOT in evaluating pavement condition based on average crack widths.

The results from this study suggest that improvements in both construction and in the concrete mix are needed. Given that MDOT is moving towards JPCP as it's standard pavement type, premature mid-slab cracking and spalling must be avoided. High PCC placement temperatures (>80 °F), especially during morning hours on hot summer days, should be avoided as premature transverse cracking can be expected. Nighttime paving would help reduce this problem.

The development of surface distress (transverse cracking, spalling and faulting) over time on OGDC pavements should be closely monitored and recorded. This will provide a valuable database for MDOT to develop performance-based specifications for either JRCP or JPCP pavements along with their related construction methods and materials.

1.0 INTRODUCTION

1.1 Overview and Background

In the early to mid 1980's the Michigan Department of Transportation, MDOT, changed the standard specifications for materials used for base courses in its typical jointed reinforced concrete pavements. Prior to that time, the standard base material was described as Dense Graded Base Course (DGBC). The new material has been defined as Open Graded Drainage Course (OGDC). Table 1.1 shows MDOT's use of OGDC materials by year since 1980. A complete listing of all MDOT projects with OGDC bases is found in Appendix A, including number of lane miles, where they are located, and when they were constructed.

Dense Graded Base Course was used exclusively in the early days of road building. The objective of using DGBC is to use a particle size gradation which, upon compaction, results in a very dense layer with low void ratio, providing stability and support for the PCC pavement. It is known that the lower void ratio and generally higher fines content of dense graded aggregates result in higher moisture contents along the bottoms of slabs, and associated delayed drainage of the pavement system. Field evaluations have suggested that presence of water in the pavement system is the main cause for initiation and development of many types of distresses. The distresses can be structural and material related such as D-cracking, ASR, pumping and frost heave.

In response to the apparent relation between drainability and pavement distresses, a second characteristic for the base came into being; namely that the base should allow all moisture that finds its way beneath the PCC slab to drain away as rapidly as possible. This perspective lead to the use of OGDC gradations.

Various OGDC gradations have been studied in Michigan since the first constructions in 1980. In mid-1980, a job specific Special Provision allowed the use of what was termed 6A modified, 9A, or 17A modified gradations. These gradations were 100% crushed and possibly stabilized using asphalt cement. Later that year, the 100% crushed requirement was reduced to 90% when the asphalt treatment was required.

In 1982, a new peastone OGDC gradation was added. The previous gradation for OGDC was revised from: 0-30% passing the #4 sieve and 0-5% passing the #8 sieve to: 0-8% passing the #4 sieve. This eliminated the finer side of the previous gradation. Also, the LA Abrasion value was incorporated limiting LA to 50 maximum.

During early 1983, the OGDC gradations were named 5G, 8G (based upon a modified 21AA standard dense graded aggregate, or the PennDOT OGS gradations), and 34G. Each of these gradations was modified on certain individual sieves and percent crushed to address problems encountered from one project to the next. The 8G was kept as drainable as possible by not allowing either asphalt or portland cement treatment.

In 1984, MDOT adopted an open graded drainage course as the standard base course. The "1984 Standard Specifications for Construction" was the first time OGDC gradations (5G, 8G, and 34G) appeared in the MDOT Standard Specifications to be used for bases and underdrains.

Through the rest of the 1980's these gradations remained essentially the same. By the time the 1990 Standard Specifications were distributed, a new 3G for bicycle paths and a 34R for underdrains were added to the book. During the early 1990's, the open graded gradations have undergone small changes, including requirements on construction practices. In particular, several versions of 3G Modified were experimented with an attempt to increase stability and pavement support without sacrificing drainability.

The 1996 Standard Specifications list four OGDC gradations: 2G, 3G, 5G, and 34R. The 2G is a new name for one of the 3G Modifieds mentioned earlier, while the 8G and the 34G have been deleted. The 3G is used as an un-stabilized OGDC. The 2G is similar to 3G except that 2G is coarser on the #8 and #30 sieves and is treated with either asphalt or portland cement. The 2G option uses 4 inch (100 mm) underdrain pipe with asphalt stabilization, and 6 inch (150 mm) pipe with the cement treated gradation. Specific construction practice differences for 2G versus the 3G are covered in Section 303 of the 1996 Standard Specifications. A new gradation being evualuated, 350AA (modified 21AA), is intended to be between the OGDC and DGBC gradations. The gradation, 350AA, gets its name from its required permeability of 350 ft/day. Table 1.2 shows the gradation bands for the current aggregates.

The sources of all OGDC gradations are allowed to consist of natural aggregates, iron blast-furnace slag, or reverbertory-furnace slag meeting the grading and physical requirements of Tables 902-1 & 902-2, respectively in the 1996 Standard Specifications. The maximum LA Abrasion requirements were changed from 50 % to 45 % for the present gradations and the percent crushed requirement has become more thoroughly defined in the 1996 book.

1.2 Problem Statement

Approximately 10 % of the projects that have been constructed with the new OGDC materials have a relatively high rate of distress development. The distresses observed have typically been premature transverse cracking as well as slightly accelerated faulting and spalling. This premature development of distress has resulted in the initiation of this study to investigate the factors that may be causing them.

In order to evaluate the effect of OGDC on the performance of PCC pavements in Michigan, 14 test sections have been reviewed in detail considering the effects of the following interacting variables:

1. *Concrete*: compressive strength, split tensile strength, elastic modulus
2. *Drainage system*: with or without underdrain, condition of drainage structure
3. *Shoulders*: shoulder type and intermediate joint design
4. *Base material*: OGDC, DGBC, type and gradation of aggregate, drainability.
5. *Subbase condition*: gradation, drainability, apparent degree of saturation.
6. *Traffic conditions and loading*
7. *Paving conditions*: temperature, humidity, time of year, curing of PCC, how soon construction and regular traffic allowed on.
8. *Pavement*: slab geometry and thickness

1.3 About This Report

Chapter 2 of this report summarizes the project objectives and scope of work. Chapter 3 discusses experimental design including selection criteria for the test sections. Chapter 4 covers the analysis of the test sections including summary tables. In Chapter 5 conclusions and recommendations are presented. Chapter 6 contains the project reference list.

A large number of appendices are included in a separate volume for this study. The mountain of compiled data, distress plots, photo logs from field testing, and laboratory testing results are contained within the various appendices. The appendices also contain the project literature review.

Table 1.1 Summary of OGDC Construction in Michigan by year.

Year of Construction	Lane Miles Constructed
1980	1.9
1981	0.0
1982	0.2
1983	22.1
1984	113.0
1985	38.5
1986	92.5
1987	68.9
1988	52.4
1989	38.1
1990	49.1
1991	45.7
1992	39.4
1993	33.0
1994	10.4
1995	44.9
1996	N/A
1997	N/A
Total miles of OGDC	650.0

Table 902-1 Grading Requirements for Coarse Aggregates, Dense-Graded Aggregates, and Open-Graded Aggregates 1996

Material Type	Class	Item of Work by Section Number (Sequential) (a)	Sieve Analysis (b) (MTM 109) Total Percent Passing									Loss by Washing (b) (MTM 108) Percent 0.075 mm
			50 mm	37.5 mm	25.0 mm	19.0 mm	12.5 mm	9.5 mm	4.75 mm	2.36 mm	0.60 mm	
Coarse Aggregates	4 AA		100	90-100	20-55	0-15		0-5				1.5 max.
	6 AAA			100	95-90	60-85	30-60		0-8			1.0 max.(c)
	6 AA	601,603,706,708,806		100	95-100		30-60		0-8			1.0 max.(c)
	6 A	205,401,402, 601,706,806										
	17 A				100	90-100	50-75		0-8			1.0 max.(c)
	26 A	706,712				100	95-100	60-90	5-30	0-12		3.0 max.
	29 A	506					100	90-100	10-30	0-10		3.0 max.
Dense-Graded Aggregates	21 AA	302,503		100	85-100		50-75			20-45		4-8(d)(f)
	21 A	302,503										
	22 A	302,306,307,503			100	90-100		65-85		30-50		4-8(d)(e)(f)
	23 A	306,307			100			60-85		25-60		9-16(f)
Open-Graded Aggregates	2 G	303(g)		100	85-100		40-70			0-10	0-8	5.0 max.
	3 G	303,304		100	85-100		40-70			0-30	0-13	5.0 max.
	5 G	205		100			0-90		0-8			3.0 max.
	34 R	404					100	90-100		0-5		3.0 max.

Table 1.2 Specification Ranges for Concrete Pavement Bases in Michigan. 1996 Standard Specification for Construction

2.0 PROJECT OBJE CTIVES AND SCOPE OF WORK

2.1 Project Objectives

The project objectives have somewhat evolved since the inception of this project. The resulting project objectives, as modified from the original proposal, are as follows:

- To identify if OGDC is playing a significant role in the types of premature pavement distresses observed.
- To analyze in detail the structural and serviceability performance characteristics of relatively new pavements in Michigan. Specifically, to identify sections constructed on OGDC which have either performed relatively poorly or well and compare them to similar DGBC sections, attempting to identify key trends and any differences in behavior.
- To identify any other factors which may be responsible for observed premature deterioration at the selected test sites.
- To find ways of identifying sections which are deteriorating at relatively rapid rates.
- To provide recommendations as to future work and methods to improve performance of the next generation of concrete pavements in Michigan.

2.2 Scope of Work

The scope of work as outlined in the original proposal has also evolved since the inception of the project as the research progressed. An outline of the work conducted is as follows:

Phase 1: Identification of performance and behavioral trends in OGDC and DGBC Sections.

1. Obtain PMS Summary data for all OGDC sections placed in the recent past. Review the data in terms of transverse cracking and spalling as a function of time and control section or construction contract limits.

2. Obtain PMS Summary data for all DGBC sections placed in the recent past. Review the data in terms of transverse cracking and spalling as a function of time and control section or construction contract limits.

3. Obtain Ride Quality Index (RQI) data on the sections from above and track trends as a function of time and control section or construction contract limits.

4. Obtain traffic data, and identify sections which have performed relatively poorly or well.

5. Identify the sections to be studied in detail by reviewing data from above and working with MDOT personnel.

6. Detailed structural and serviceability evaluation consisting of:

   A. Distress and drainage surveys, mapping and quantifying observed distresses and notable features.

   B. Falling Weight Deflection, FWD, testing on most study sections. The testing was performed at mid-slab, corners, and edges at morning, noon, and mid afternoon.

   C. Dynamic Cone Penetration, DCP, testing at all test sections with the U.S. Army Corps. of Engineers device.

   D. Core sampling of the pavement concrete for laboratory analysis.

   E. Sampling of base, subbase, and subgrade/embankment layers for laboratory analysis.

7. Evaluate all above data, prepare phase 1 report, and recommend direction for phase 2.

Phase II: Identification of OGDC and Other Factors Responsible for Observed Premature Distresses

1. Review of historical records for environmental conditions during placement for the selected test sites.

2. Investigation of sections which exhibit transverse cracking very early in their design lives.

3. Determination of primary factors causing premature distresses observed.

4. Preparation of final report for the project.

3.0 EXPERIMENTAL DESIGN

3.1 Selection of Test Sections

More than 650 lane miles of concrete pavement in Michigan have been built on OGDC since 1980. This large investment in OGDC systems merits a careful investigation of the influence of OGDC on pavement performance. Consequently, representative study sections must be chosen to provide evidence of the influence of the base course on the performance of the entire system. A complete listing of all OGDC pavements in Michigan is found in Appendix A.

Historical records, and data from the pavement management system (PMS) consisting of distress index and ride quality index data (RQI) can be used to give some indications of distress development in various pavements. However, these cannot replace detailed field evaluation and laboratory testing. Still, in a limited duration study, field evaluation of pavements is only possible at one point in time, making it difficult to describe the development of distresses. For this reason, it is valuable to choose study sections that represent long-term performance, while also studying performance of other pavements early in their service lives.

Since Michigan has only used OGDC systems since the early 1980's, "longer term performance" in this study refers to pavements that have been in service for at least 10 years.

In order to evaluate the longer-term performance of OGDC pavements, six pavements supported by OGDC were selected representing a wide range of distress levels (as characterized by transverse cracking, spalling, and faulting). Three additional sections on Dense Graded Base Courses (DGBC) were chosen for comparative purposes. Initially, selections were made by reviewing PMS data, historical records, and recommendations by the MDOT TAG. Of particular interest in the historical records were the gradation specifications of the base course materials. In addition, efforts were made in site selection to minimize the effects of other variables such as traffic volumes, slab length, and pavement age. The final selections were made after walk-throughs in the field, which ensured that representative test sections were chosen for the investigation.

The studied sections range from 10 to 16 years in age, with all but 2 being between 10 and 13 years old. All sections, but one, have 41 ft. transverse joint spacing. The remaining

section has 44 ft. joint spacing. All the JRCP projects have 12 ft. wide traffic lanes, and 9 in. thick concrete slabs supported on a 4 in. thick base course. The JPCP project has a 15-17 ft. joint spacing; 14 ft. widened truck lanes and 12 in. thick PCC slab. All have concrete shoulders. In some cases intermediate shoulder joints were found. This design is believed to have initiated and promoted transverse cracking. Traffic ranges from 178,900 to 455,300 total lane ESAL's per year in the truck lane. While this does suggest considerable variation in traffic levels, none of these sections represent extremes in traffic volume.

All of the study sections except one were selected along the I-69 corridor between Port Huron and Lansing. The additional section is located on I-475 in Flint, within a few miles of I-69. This close proximity helps to keep climatic effects such as number of freeze-thaw cycles on the pavements relatively constant for the study sections. The nine chosen sections for the longer-term performance study are shown in Table 3.1 below. Detailed site information on each test section is found in Appendix B.

Table 3.1 *Pavements selected for the longer-term performance study.*

Route	CSN-Job#	Location	Job Length miles	Year Constructed	Base* Type
I-69	19042-02233A	EB,Webster Rd to Upton Rd	3.6	1987	8G
I-69	19042-24680A	EB, Chandler Rd to Webster Rd	2.6	1986	8G
I-69	19043-02234A	EB, Airport Rd to US27	3.1	1981	22A
I-69	19043-02234A	WB, Airport Rd to US27	3.1	1981	22A
I-475	25132-06582A	SB, Steward Rd to Coldwater Rd	2.5	1981	22A
I-69	44044-18804A	WB, M-24 to East of Wilder Rd	3.7	1984	8G
I-69	77023-21586A	EB, M-19 to GT&W RR	10.4	1984	8G
I-69	77024-17988A	EB, Cox-Doty Drain to M-19	5.6	1984	8G
I-69	77024-20821A	EB, Countyline to Cox Doty	5.8	1984	8G

* This is the base as specified per construction plans. Sieve analysis may show that the base fits a different gradation.

The study of newly constructed sections includes three sections that were two years old at testing, and two sites that were under construction at time of testing. The three sections that were two years old at testing are located on I-94 near Watervliet. They were selected because premature distress in the form of transverse cracking had been observed, and it was suggested, that the OGDC could be a contributing factor.

The two sections under construction at the time of testing were similar in design to the three sections on I-94, and allowed for instrumentation of the slabs and observation of the construction process. Table 3.2 lists the four sections studied in the new construction study.

Table 3.2 Pavement sections selected for the new construction study.

Route	CSN-Job#	Location	Job Length miles	Year Constructed	Base Type
I-94	11017-32516A Sec A	EB, East of Park Rd	2.0	1995	3G
I-94	11017-32516A Sec C	EB, West of Carmody Rd	1.5	1995	3G
I-94	11017-32516A Sec D	WB opposite sections A-C	5.0	1996	3G
I-96	47065-28215A	EB & WB, East of D19 and West of Dorr Rd	3.6	1997	3G 350AA*

* This was a test section in the WB direction

3.2 MDOT PMS Data

Pavement management system (PMS) data were used to assist in the selection of test sites. Part of PMS is a distress index evaluated for every tenth of a mile of pavement. The distress index is a number that ranges from 0 to 50, where 0 represents a distress free pavement and 50 represents a service threshold. Distress index is used to quantify the amount of distress that is present. It takes into account transverse and longitudinal cracking, damage at joints and any mud jacked slabs or shattered slabs that might be present. All of this distress is then quantified to obtain the distress index.

In this study distress index was used to look at potential test sections and specific test sites within candidate sections. The data were reviewed to locate sections of low, medium and high distress. Further, the data also provided an understanding of the types of distress present and a measure of the variability in performance within test sections. As an example Figure 3.1 shows the 1995 distres index data for control section 77024 eastbound. The two test sites chosen from this control section were at milepost 1.3 to 1.4 and 7.5 to 7.6. It is quickly seen in the figure that significant differences in performance were expected. Furthermore, it is noted from the figure that a sudden drop in distress index occurs near milepost 5.8. This location represents the border between two separate paving contracts. Review of the PMS data has shown that it is not uncommon to see different distress development patterns associated with individual paving contracts. The 1995 distress index data for the control sections studied is found in Appendix F.

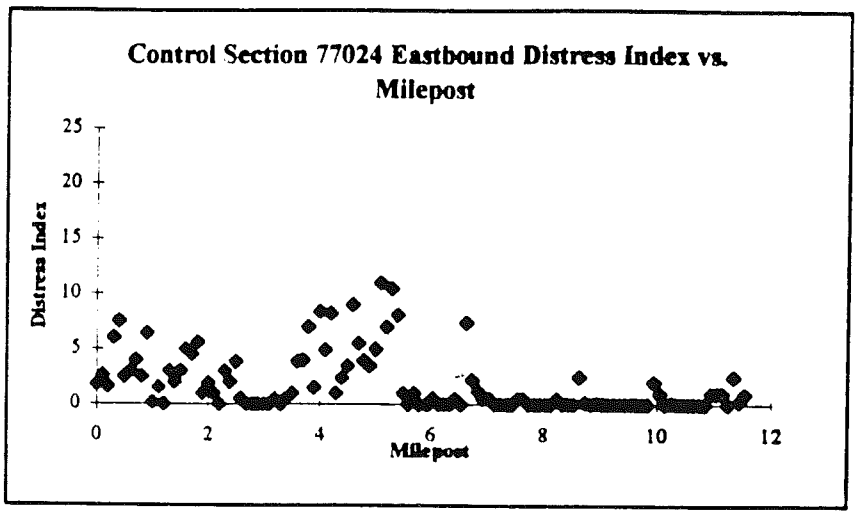

Figure 3.1 *The PMS data for control section 77024 EB.*

In addition to the distress index, Ride Quality Index (RQI) data were also reviewed. RQI is a measurement of the pavement's surface profile. This information is obtained by using a profilometer driven down the right wheel path of a lane. This change in surface profile is then quantified as RQI. The RQI is calculated for every tenth of a mile.

By having RQI data from 1992 through 1995 available, it has been possible to review the rate of change of the surface profile over time. RQI was the only available measure of deterioration rate, and was thus a valuable tool in selecting a site. As an example two pavements with similar RQI values can be distinguished by their deterioration rates. One would be much more concerned over a pavement that is deteriorating rapidly, then one that developed some roughness early in its life but has been stable since.

In the figures below one can see the RQI data and the RQI growth rate for control section 77024 EB. Figure 3.2 shows the RQI data for 1992-1995. The mileposts tested on this control section were 1.3 to 1.4 and 7.5 to 7.6. This figure shows that the these two locations have very similar RQI values.

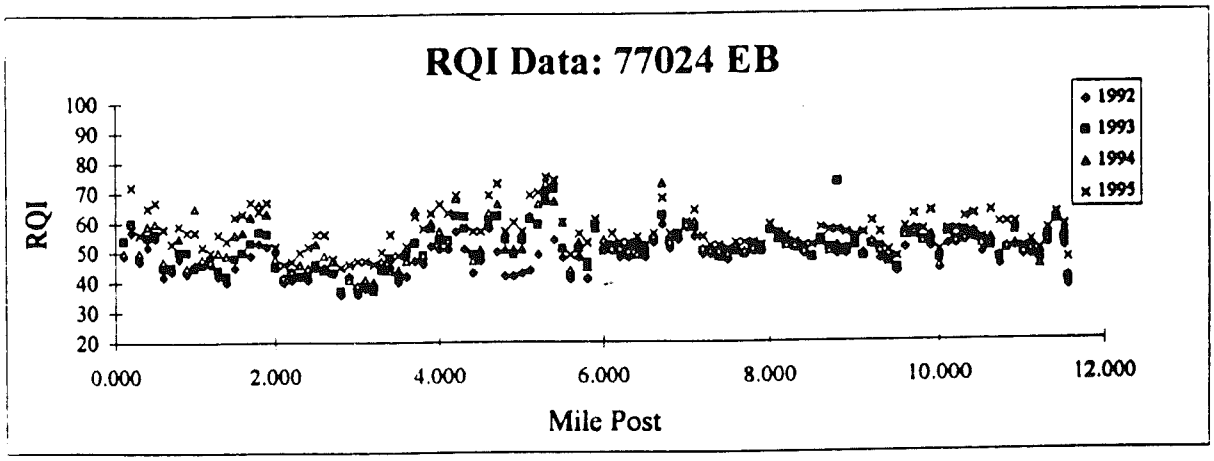

***Figure 3.2** RQI data for Control Section 77024 EB*

In Figure 3.3 below, the growth rate of the RQI data is shown. This figure again shows clearly the border between the two paving contracts at milepost 5.8 which agrees with PMS Data. RQI data for each of the selected control sections are found in Appendix F.

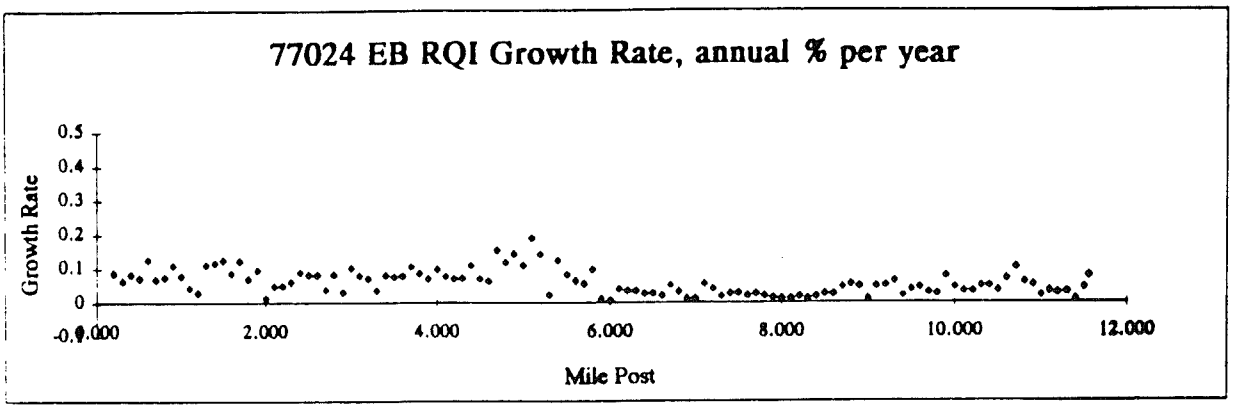

Figure 3.3 RQI Growth Rate of the RQI data for Control Section 77024 EB

3.3 Historical Records

Through the use of historical records, additional information about potential test sites was obtained. The historical records contain the mix designs used, base and subbase gradations, weather during construction, and inspector's daily reports that give detailed information about construction. The historical records complement the information obtained from PMS, and can highlight potential causes of distress development.

3.4 Field Condition Survey

In order to finalize site selection, a field condition survey was performed. This survey was a walk through of a potential section to verify information obtained in PMS and the historical records. The types of distress present and their severity are investigated further during the on site survey. Additionally, the drainage of the site and the traffic volume present at this time were observed. After the field condition survey, final decisions were made as to the suitability of a given test location.

3.5 Field Testing Procedures

In order to quantitatively evaluate the performance and condition of a selected test site, both field and laboratory testing programs were conducted. The data gained from these investigations, combined with the PMS and historical records were used to compare and contrast the various pavement systems.

Within each selected control section, a 500ft. (1000 ft. in some cases) long test section in the truck lane was chosen as representative of typical distresses found along the contract limits. Where possible, special features such as inclines, culverts, overpasses, high degree of curvature, and ramps were avoided. Testing typically began early in the morning and continued throughout the day.

Once the 500 ft test section was selected based on a preliminary walk-through of the site, lane closure was established. The pavement was then marked to indicate locations for core samples and Falling Weight Deflectometer (FWD) measurements. Once the FWD and coring crews were mobilized, a thorough distress survey of the site was performed, along with a visual drainage survey and photographic record. Distress surveys included locations of cracks and crack widths, spalls, faulting and other distresses. Coring and FWD locations were recorded.

Falling weight deflectometer testing started as soon as lane closure was available and the site was marked. FWD testing was repeated in the afternoon. On some sites, when weather conditions were changing rapidly, FWD testing was performed three times during the day.

As soon as the FWD crew proceeded past the first coring location, the drilling team began taking concrete core samples. Core drilling was followed by DCP measurements and aggregate sampling beneath selected core holes. In the following sub-sections, each of the field testing methods and procedures are discussed in detail.

3.5.1 Site Photos

Photos of each test section were taken to create a visual record of each site at the time of testing. The photographic record includes overview photos showing the contour of the land and the general layout of the site. In addition, photos of each tested slab were taken. These photos show locations of distresses, coring and FWD locations, and transverse joints. Special features of the sites were also recorded, such as close-up views of drainage structures, core holes, and distresses. In Appendix D, a few representative photos from each site have been included to give a quick visual representation of the various test sections.

3.5.2 Distress and Drainage Surveys and Crack Width Measurements

Distress surveys for each test site were conducted showing in detail the locations of core holes, FWD tests, transverse joints, transverse and longitudinal cracks, spalling, faulting, and other surface distresses and notable features. Cracks were measured for width and length. A crack comparator card was used to measure average crack widths to the nearest 4 mils (0.1 mm). On a few test sections, faulting was measured to the nearest 4 mils (0.1mm) using a Georgia faultmeter. Other features noted include utilities, delaminations due to high steel, and significant pop-outs. A portion of a typical distress survey can be seen in Figure 3.4.

Drainage surveys were conducted to detect any potential water-related problems in the pavement systems. Notations included locations and conditions of drain outlets, clogging of drain outlets, standing water in the ditches, growth of swamp vegetation in ditches, condition of drainage structures in the median and other notable features. The distress surveys are presented in Appendix C.

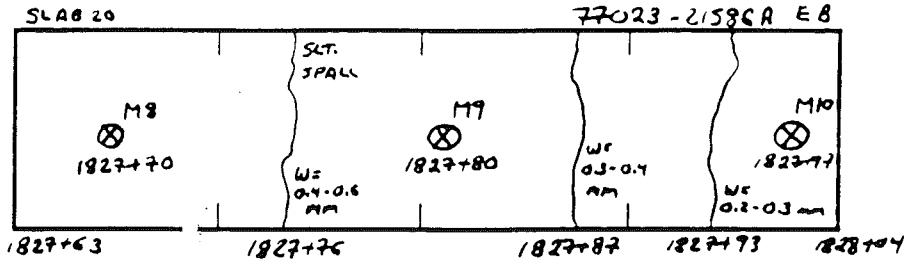

Figure 3.4 A typical distress survey from section 77023-21586A EB .

3.5.3 Concrete Coring

Concrete coring was conducted in accordance with ASTM procedure C 42-94 (by MDOT personnel). The cores were labeled with an identifying number and station location. Concrete was cored for laboratory determination of compressive and split tensile strength, elastic modulus, and pavement thickness determination. In addition, the coring locations provided access to the underlying foundation for soil sampling. A minimum of six cores were taken from undamaged areas in the middle of slab panels. Three of these cores were used for compressive strength and elastic modulus determination, and the other three for split tensile strength. Additional cores were taken from cracks and transverse joints to evaluate dowel bar conditions and to make qualitative observations of the crack surfaces.

3.5.4 DCP Testing

Dynamic cone penetrometer testing was performed using the U.S. Army Corps of Engineers DCP apparatus. DCP tests were performed at 5 to 6 locations on each site at the mid-slab core holes. DCP values were recorded as millimeters of travel by the DCP shaft versus blowcount on the anvil. One blow refers to dropping a 10.1 lb. (4.52 kg) weight onto an anvil from a standard height of 22.6in. (565 mm).

Correlations are found in the literature to relate mm/blow for DCP to California Bearing Ratio (CBR). The correlation recommended by the U.S. Army Corps of Engineers is:

$$CBR = 292/DCP^{1.12} \qquad \text{(Metric)}$$

The correlated CBR values have been calculated for this project's data in Appendix I. It should be noted, though, that the correlations may not be well suited for the soil types encountered in this study. Thus, the CBR correlations should be considered only provisional.

The value of DCP measurements is that they provide a direct measure by which to compare the stiffnesses of different core holes and test sites on a relative basis. Figure 3.5 shows the variation of average base and subbase DCP values over a 500 ft. (152.4 m) test section. Base values reported here are mm/blow values averaged over a depth of 0 to 3 in. (0 to 75 mm) below the concrete. Subbase values are averaged from 6 to 10 in. (150 to 250 mm) below the concrete. Variations over the job length are qualitatively representative of differences in foundation stiffness. It should be noted that the lower DCP values for the base course are likely caused by a lack of confinement after removal of the weight of the core.

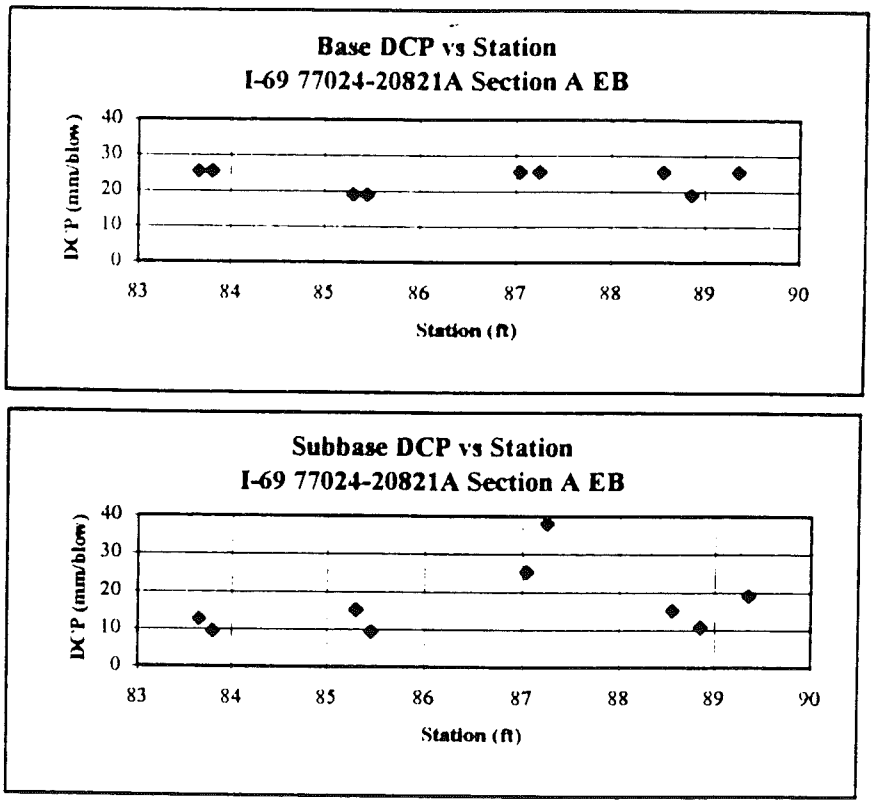

***Figure 3.5** DCP versus station for 77024-20821A Sec A EB*

3.5.5 Soil Sampling

Samples were taken from the base, subbase, and subgrade of each mid-panel core location for each test section using a hand held soil auger. If embankment material was present, samples were obtained for records along with subbase materials. On some sections subgrade samples could not be obtained. The samples labeled and taken to the laboratory for loss by wash and gradation analysis. Based on the resulting gradation curves filter criteria and foundation permeability were calculated.

During soil sampling, the thickness of the various foundation layers were recorded. The pavement system profiles can be found in Appendix B. The distinction between subbase and subgrade was sometimes unclear, and the depth of the transitions were estimates.

3.5.6 FWD Testing

Falling Weight Deflectometer data were obtained using the MDOT operated KUAB system. The system is monitored with 1 load sensor, 9 deflection sensors, and 2 temperature sensors for air and pavement surface temperature. Figure 3.6 outlines the system setup.

Typically, FWD data were obtained on 5 slabs at the corner, midslab and edge. In addition, a selected number of transverse cracks were tested. At each location, FWD data were obtained at three load levels at transverse cracks and transverse joints. The latter was to evaluate potential loss of support underneath the slab at discontinuities.

As researchers have recommended that FWD testing performed be in the early morning hours where the pavement is curled upwards, FWD testing was performed as soon as when traffic control allowed it. In addition, FWD testing was repeated later in the day to evaluate any effect on transverse joint and crack load transfer.

Falling Weight Deflectometer Layout

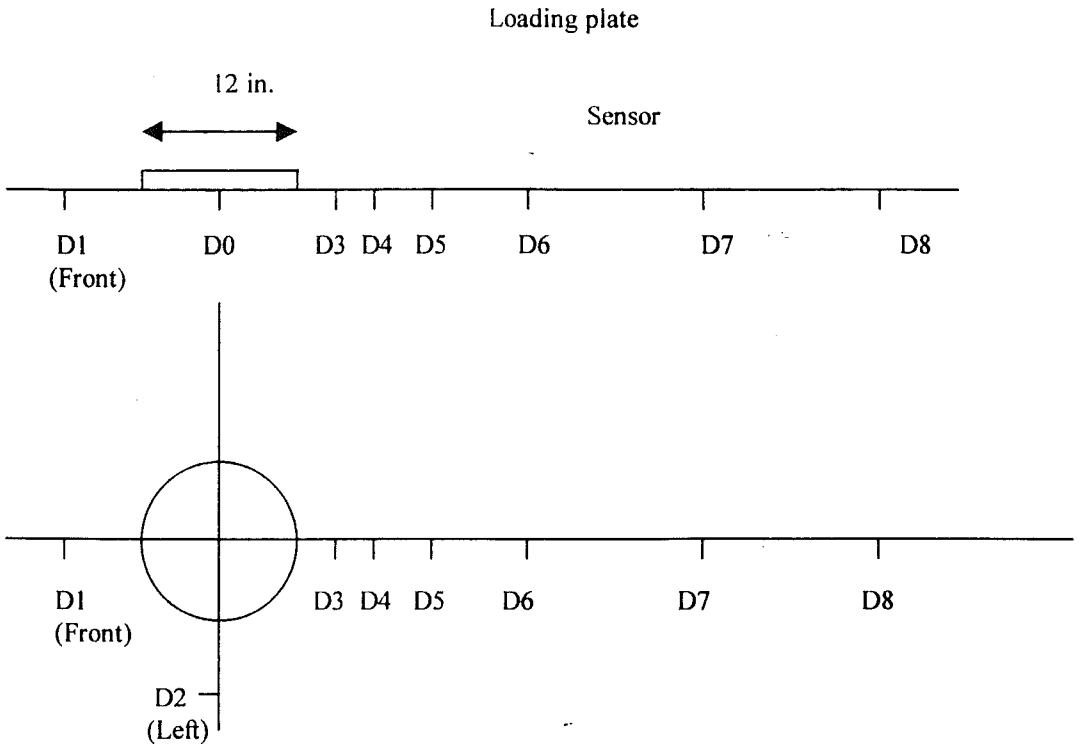

Sensors	Location from the plate center (in.)
D0	0
D1 (front)	12
D2 (left)	12
D3	8
D4	12
D5	18
D6	24
D7	36
D8	60

Figure 3.6 *Sensor location on MDOT FWD testing equipment, KUAB.*

Load transfer efficiency, LTE, is defined as the deflection ratio between the unloaded panel and the loaded panel. 100 % LTE is achieved when the deflection on the unloaded panel equals the deflection on the loaded panel. 0 % LTE is achieved where is no deflection of the unloaded panel. The load transfer efficiency can be obtained by either dropping the load before or after the discontinuity. The terminlogy used defines the loading before as loading of the approach slab and the loading after as loading of the leave slab. Further, when calculating the joint load transfer efficiency *AASHTO Guide for Design of Pavement Structures* recommends using deflections obtained at an equal distance from the discontinuity, which is also in agreement with research performed by Owusu-Antwi et al. (1995 TRB). It is believed, that similar assumptions are valid for transverse cracks, and therefore only data obtained from sensors D0 and D1 or D0 and D4 are used to calculate load transfer efficiency. Furthermore, the load is applied about 2 feet from the longitudinal joint between shoulder and slab in the outer-wheel path. Results from FWD are found in Appendix J.

3.6 Laboratory Testing

Once soil samples and concrete cores were obtained from the selected test sections, they were taken to the laboratory for testing. The lengths of six cores were measured before cutting with a diamond blade to establish two flat surfaces. The smallest possible amount was cut to maintain the longest possible specimen. Three of the cores were then capped according to ASTM C 617-94, with sulfur capping compound to ensure plane and level surfaces at both ends. The capped length of the cores were then measured. The specimens were now ready for compression testing. The other three cut cores were then measured in preparation for split tensile testing.

Soil samples were placed in zip-loc bags and sealed. Upon returning to the laboratory, the soil samples were oven dried. Once dry, the soil samples were ready for loss by wash testing and gradation testing. Loss by wash and Sieve Analysis were conducted according to ASTM C 117-95 and C 136-95a respectively.

3.6.1 Concrete Properties

Three specimens per site were tested in compression according to ASTM C 39-94. The elastic modulus was determined according to ASTM C 469-94. The remaining three cores

were tested for split tensile strength according to ASTM C 496-90. Appendix G shows the concrete properties for all sections tested.

3.6.2 Aggregate Gradation - Loss by Wash and Sieve Analysis

Loss by wash was performed on the dense graded base course samples, as well as subbase and subgrade samples from all sections. This test was performed according to ASTM C 117-95. Sieve analysis was performed in accordance with ASTM C 136-95. After much of the sieving was completed, it was observed that ASTM limits on amount of material retained on a sieve had been exceeded for a number of samples. The potential impact of this error was of concern to the research team. For this reason, sieve analysis was repeated for about 20 samples where the limits had been exceeded. The results from this sieving were then compared to the original sieving results. It was found that there was no significant impact from exceeding sieve weight limits. This gave the research team the needed confidence to continue analysis with the existing data.

3.6.3 Filter Criteria, Hazen Permeability

After loss by wash and sieving were performed on the aggregate samples, and filter criteria were calculated. The criteria used and its results are shown in Appendix H.

3.6.4 Resilient Modulus Testing

The LTPP Protocol P46 Resilient Modulus of Unbound Granular Base/Subbase Materials and Subgrade Soils (1996) was followed as closely as possible throughout this portion of the laboratory investigation. This procedure is based on AASHTO T292-91I *Resilient Modulus of Subgrade Soils and Untreated Base/Subbase Materials*. Sample preparation was done according to the specifications within the P46 protocol. A split mold was constructed to house the 6 in. (152-mm) diameter by 12 in. (304-mm) high samples. The following outlines the experimental setup and laboratory techniques used.

This study evaluated two aggregate materials that are representative of those commonly used by MDOT: glacial sand and gravel aggregate and crushed limestone. These materials were selected to represent two distinct aggregate types that are commonly used as base course material under PCC pavements.

The glacial aggregate was obtained from the Searles Quarry near US 27 in St. Johns, MI. As with most glacially derived aggregate it contains a wide range of mineral types including quartz, feldspar, basalt, granite and limestone with quartz as the dominant constituent. As the glacier moved, the incorporated materials underwent considerable crushing which eliminated weaker particles while rounding the stronger material. Consequently, glacial aggregate tends to consist of strong, highly resistant aggregate. However, the glacial grinding action also produced semi-rounded or subangular particles, which tend to have poor interlock characteristics. Thus some artificial crushing of the glacial aggregate was required to increase its angularity and improve its mechanical properties. The glacial aggregate used in this study underwent partial crushing, producing aggregate having one to two fractured faces as required by MDOT specifications. This significantly improves the mechanical behavior of the aggregate compared to a completely rounded aggregate source.

The crushed limestone material was obtained from the Thompson – McCully Quarry located near Newport, MI. This aggregate, composed of dolomite and limestone, was both blasted and crushed, and therefore had 100 percent crushed faces. It is noted that when the aggregate was received at MTU, all the particles were coated with fines and bound together in the canvas shipping bags. Considerable efforts were expended to sieve the material, separating the fines from the coarser aggregate particles.

Three MDOT gradations were evaluated in this research. The first gradation evaluated is the dense-graded 21AA which is representative of the traditional gradations used in PCC pavement prior to the conversion to drainable bases. It is relatively well graded with 5% fines passing the 0.075 mm sieve. While this gradation provides a dense base, it is also relatively impermeable. To evaluate aggregate gradations more representative of the open-graded drainage courses used by MDOT, a representative 3G gradation was used. This gradation does not allow for any material passing the 0.075 mm sieve and is referred to as "open graded." The third gradation selected for study was the new 350AA, which includes approximately 2.5% fines with an anticipated permeability of 350 feet per day.

The gradations for each of the three bases evaluated in this study are provided in the table below. The information in the table includes the percent material passing each sieve and the mass of material retained on each sieve needed to produce the test specimens. It is noted that MDOT gradation specifications provide a range of allowable percent passing for each sieve reflecting material variability in the field. MTU worked with MDOT to select the actual percent passing each sieve for this laboratory analysis to be representative

of a mid-range gradation. After selection of the target values, the gradation of each test specimen was precisely controlled.

Table 3.3 Percent passing by weight for the MDOT 21AA, 350AA, and 3G gradations.

	Percent Passing by Weight							
Sieve (mm)	25.4	12.7	4.75	2.36	0.6	0.075	pan	Total
21AA								
Percent Passing (%)	92.50	62.50	42.50	32.50	17.50	5.00	0.00	
mass retained (g)	988.81	3955.25	2636.8	1318.4	1977.6	1648.0	659.2	13184.1
350 AA Middle								
Percent Passing (%)	95.00	55.00	32.50	22.50	10.00	2.50	0.00	
mass retained (g)	659.21	5273.66	2966.4	1318.4	1648	988.81	329.6	13184.1
3G Open								
Percent Passing (%)	95.00	55.00	27.50	15.00	7.50	0.00	0.00	
mass retained (g)	659.21	5273.66	3625.6	1648.0	988.81	988.81	0.00	13184.1

Three samples were made for each gradation with each material type. This produced a total of 18 samples that were tested in the following moisture states: dry, drained and un-drained. The dry condition is defined as the 2 - 3 % moisture content present in the aggregate immediately following sample compaction. This moisture condition is representative of a newly placed base course in the field subjected to minimal traffic and no exposure to moisture.

The second moisture condition investigated was the drained condition. After completing testing in the dry condition, the drained condition was achieved by completely saturating the sample from the bottom up for 12 hours and then allowing it to drain for two hours prior to testing. This moisture condition was designed to simulate a base course connected to a working drainage structure that allows water to freely flow through gravitational

forces alone. A drainage period of two hours is the recommended drainage time for open graded material as defined by Cedergren and the FHWA.

Once testing was completed in the drained condition, the sample was again completely saturated, but this time all the drains were closed during testing. A specimen tested under this situation is referred to as being in an undrained moisture condition. This testing was designed to represent a base course in a completely saturated condition. Testing under these conditions significantly reduces the resiliency of the aggregate base course. Pore water pressure was monitored throughout the testing sequence to obtain B parameter results (Note: the B parameter = u/σ_3 where u is the pore water pressure and σ_3 is the confining stress). When the pore pressure was equal to the cell pressure the B parameter is equal to unity, therefore indicating a saturated state exists.

Compaction was accomplished using an electric Makita demolition hammer. The hammer weighed 20.7 lbs. (9.4 kg.) and was capable of 2000 blows per minute. The material was compacted in six, 2 in. (50-mm) lifts to achieve a total sample height of 12 in. (305 mm). A 0.022 in. (0.55 mm) rubber membrane was placed between the mold and granular material to help support the sample throughout the testing sequence. The amount of time required to compact each lift varied according to the material type and required density. The optimum densities were obtained from MDOT and verified by MTU using the modified proctor test method. Table 3.4 summarizes the densities typical of the aggregate and gradations used in this study.

Table 3.4 *Typical modified proctor densities.*

Material TypeType	**Gradation**	**Optimum Density (g/cm^3)**	**95 percent of Optimum (g/cm^3)**
Quarried Limestone	21 AA	2.26	2.14
	350 AA	2.08	1.98
	3G	2.05	1.95
Glacially Derived	21 AA	2.30	2.19
	350 AA	2.13	2.02
	3G	2.10	1.98

Testing was accomplished with a closed loop servo-hydraulic MTS testing system. MTS technicians and MTU researchers calibrated the system prior to testing. The MTS system had a 5.5 kip. (24.5 kN) load cell and a 22 kip (98 kN) frame. Table 3.5 presents the testing sequence established in the P46 protocol, including the confining pressure,

maximum axial stress, cyclic stress, contact stress, and number of load applications for each step. Each specimen in each moisture condition was subjected to this sequence.

Table 3.5 *Resilient Modulus Testing sequence used for this study.*

Step Number	Confining Pressure		Maximum Axial Stress		Cyclic Stress		Contact Stress		No. of Load Applications
	kPa	psi	kPa	psi	KPa	psi	kPa	psi	
0	103.4	15	103.4	15	93.1	13.5	10.3	1.5	500
1	20.7	3	20.7	3	18.6	2.7	2.1	0.3	100
2	20.7	3	41.4	6	37.3	5.4	4.1	0.6	100
3	20.7	3	62.1	9	55.9	8.1	6.2	0.9	100
4	34.5	5	34.5	5	31.0	4.5	3.5	0.5	100
5	34.5	5	68.9	10	62.0	9.0	6.9	1.0	100
6	34.5	5	103.4	15	93.1	13.5	10.3	1.5	100
7	68.9	10	68.9	10	62.0	9.0	6.9	1.0	100
8	68.9	10	137.9	20	124.1	18.0	13.8	2.0	100
9	68.9	10	206.8	30	186.1	27.0	20.7	3.0	100
10	103.4	15	68.9	10	62.0	9.0	6.9	1.0	100
11	103.4	15	103.4	15	93.1	13.5	10.3	1.5	100
12	103.4	15	206.8	30	186.1	27.0	20.7	3.0	100
13	137.9	20	103.4	15	93.1	13.5	10.3	1.5	100
14	137.9	20	137.9	20	124.1	18.0	13.8	2.0	100
15	137.9	20	275.8	40	248.2	36.0	27.6	4.0	100

The testing software records all the relevant information for each load pulse including both the input stress levels and the resulting resilient and permanent vertical strain. Using this data, the resilient modulus of the material can be computed for each load application and the accumulated permanent deformation can be plotted. The testing software records all the relevant information for each load pulse including both the input stress levels and the resulting resilient and permanent vertical strain. Using this data, the resilient modulus of the material can be computed for each load application and the accumulated permanent deformation can be plotted. The software records all the relevant information for each load pulse including both the input stress levels and the resulting resilient and permanent vertical strain. Using this data, the resilient modulus of the material can be computed for each load application and the accumulated permanent deformation can plotted.

4.0 DISCUSSION OF RESULTS

4.1 Overview

This chapter presents the analysis of six OGDC and three DGBC sections constructed in the mid 1980's, all JRCP's. A two year old JPCP project on OGDC, which showed premature mid-slab transverse cracking, was included during the second year of this study. Three sections from this project were investigated. Thus, a total of 12 field projects were studied in detail.

The analysis focuses on the plausible causes for the observed pavement distress (i.e. transverse cracking, spalling, and faulting) with the major objective to identify if the OGDC is contributing to the formation of premature deterioration. It is important to keep in mind that pavement distresses naturally develop over time through a combination of environmental and traffic effects. In addition, low severity transverse cracking (i.e. tight crack without spalling) is a normal occurrence in JRCP. These cracks are expected to develop as the slab responds to repeated temperature changes (contraction and curling). It is the occurrence of medium and high severity cracking, with associated spalling and faulting, that are of concern because they trigger the need for repair and/or rehabilitation.

A variety of pavement evaluation techniques were used. They include: visual distress surveys, visual inspection of outlet drains, coring of PCC specimens for mechanical properties, layer stiffness evaluation using dynamic cone penetrometer, aggregate sampling for gradation and filter criteria determination, resilient modulus testing of various base materials, and falling weight deflectometer testing at joints and cracks for void detection and load transfer analysis. In addition, MDOT historical records were used to provide project information such as mix designs, paving dates and amounts, and air and concrete placement temperatures.

The amount of data gathered and the range of testing conducted on this project is substantial. The attempt of this chapter is to discuss the major findings of this study as a stand-alone document, but the reader is, where appropriate, referred to the appendix for more detail.

Table 4.1 lists key site data for the 12 projects, including the year of construction, traffic, pavement layer thickness and pavement type.

Table 4.1 Measured average pavement layer thickness, base type, joint spacing and estimated traffic.

Projects	Year Built	Estimated Traffic	Pavement Type & Joint Spacing	*Field Slab Thickness	MDOT Base Class	Subbase Thickness
		(ESAL's/Year)		in.		in.
OGDC						
I-69 CSN 77023-21586 St. Clair Co.	1984	178900	JRCP 41 ft	9.65	8G	10-14 in
I-69 CSN 77024(A)-20821 St. Clair Co.	1984	178900	JRCP 41 ft	9.45	8G Gravel	8-10 in
I-69 CSN 77024(B)-17988 St. Clair Co.	1984	195100	JRCP 41 ft	9.35	8G	10-18 in plus fill
I-69 CSN 44044-18804 Lapeer Co.	1984	243900	JRCP 41 ft	9.45	8G Gravel	8-10 in
I-69 CSN 19042(B)-24680 Clinton Co.	1986	455300	JRCP 41 ft	9.55	8G	8 in plus fill
I-69 CSN 19042(C)-02233 Clinton Co.	1987	455300	JRCP 41 ft	8.95	8G	8 in plus fill
I-94 CSN 11017-32516 Sec. A EB Berrien Co.	1995	406500	JPCP 16 ft Widened lane: 14 ft	11.65	3G (6A) Limestone	8++ in plus embankmen
I-94 CSN 11017-32516 Sec. C EB Berrien Co.	1995	406500	JPCP 16 ft Widened lane: 14 ft	11.55	3G (6A) Limestone	8++ in plus embankmen
I-94 CSN 11017-32516 Sec. D WB Berrien Co.	1996	406500	JPCP 16 ft Widened lane: 14 ft	11.75	3G (6A) Limestone	8++ in plus embankmen
DGBC						
I-475 CSN 25132-06582 Genesee Co.	1981	316200	JRCP slab length = 44 ft	8.9	22A	10 in
I-69 CSN 19043-02234 (metric Job) EB Clinton Co.	1981	374000	JRCP slab length = 41 ft	9.3	22A	8 in plus fill or sandy subgrade
I-69 CSN 19043-02234 (metric Job) WB Clinton Co.	1981	374000	JRCP slab length = 41 ft	8.9	22A	8 in plus fill or sandy subgrade

* Slab thickness correction of 0.25 in. due to PCC penetration into OGDC base.
No correction for DGBC

4.2 Pavement Distress Types and Development

Table 4.2 is a summary of the 1995 MDOT PMS distress data, listing average distress points for each of the projects, as well as the average distress points corresponding to the milepost range tested. No PMS data were available for the newly constructed sections on I-94 near Watervliet (i.e. CSN 11017). All the results and plots of distress points versus milepost are shown for the entire length of each control section in Appendix F

As seen from these results none of the projects have reached the threshold value of 50 distress points, with an average distress value for all the projects of 4.4. The average value for the OGDC's studied is 3.0 and 7.2 for the two slightly older DGBC sections. This indicates that the deterioration of OGDC pavements does not appear to differ greatly from that of DGBC sections for projects of similar traffic and age. Of the OGDC pavements, CSN 77023 has the highest average distress value of 7.9 for the entire project, and the CSN 19042 projects (B, and C) have the lowest distress values of 0.4. Clearly the 77023 and 19042 projects are performing very differently over time, and will be discussed in more detail below.

A similar conclusion is reached from the analysis of ride quality index (RQI) data based on four consecutive years of data between 1992 and 1995. RQI, which is an index related to measured pavement surface roughness, is influenced by distress development. The MDOT database RQI values versus milepost are plotted for each job in Appendix F. The plots show that the general trend for RQI vs. time is very similar for OGDC and DGBC pavements, with a tendency of OGDC pavements to be rougher early on.

Field measurements of distress, presented in Appendix C, were used to quantify transverse cracking and spalling. These results are shown versus time in Figure 4.1. Distress results for the 16 year old DGBC section, (CSN 25132), were excluded from this figure because this project was cold patched at several locations due to spalled cracks. In general, both distress types follow expected trends over time with little if any spalling development observed during the first 10 years. These results corroborate MDOT PMS findings, and they generally indicate that there is little evidence of premature (i.e. within the first 10 years of service life) deterioration of OGDC pavements. However some pavements (CSN 77023, 77024A) have developed severe spalling and faulting after about 13 years. The most plausible cause of this high level of spalling is trapped water in the subbase/subgrade and clogged outlet drains, as discussed in section 4.3. No evidence could be found that the OGDC in and of itself was a major contributor.

Table 4.2: Summary of MDOT PMS distress points measured in 1995.

Project No.	Route & Year Open	Direction	Project Length (MI.)	Mile Post Test Range	Ave. Project Distress Point	Test Section Distress Point
OGDC Projects:						
CSN-77023-21586	I-69, 1984	EB	15.283	5.9	8.1	3.96
St. Clair Co.		WB	15.229		7.6	
77024(A)-20821	I-69, 1984	EB	5.8	1.312-1.43	1.9	0.448
St. Clair Co.		WB	5.8		1.4	
77024 (B)-17988	I-69, 1984	EB	5.638	7.452-7.646	1.9	3.25
St. Clair Co.		WB	5.6			
44044-18804	I-69, 1984	EB	17.349		1.3	
Lapeer Co.		WB	17.566	1.732-1.839	2.6	0.883
19042Projects A,B,C	I-69, 1986					
Clinton Co.						
Job 24680 (B)	1986	EB	8.797	2.077-2.204	0.4	0.328
Job 02233 (C)	1987	EB	8.867	6.863-6.973	0.4	0.472
11017-32516	I-94, 1995	EB	2.02	3.924-4.019	NA	NA
Section A(EB)						
Berrien Co.						
11017-32516	I-94, 1995	EB	1.57	1.889-2.032	NA	NA
Section C(EB)						
Berrien Co.						
11017-32516	I-94, 1996	WB	5.18	3.791-3.981	NA	NA
Section D						
Berrien Co.						
Dense-Graded Projects:						
25132-06582	I-475,1981	SB	16.747	12.3	11.2	3.16
Genesee Co.		NB	16.982		9.6	
19043-02234	I-69, 1981	EB	9.2	4.943-4.980	4.6	1.32
EB (Metric Job)		WB	9.154	6.3	3.3	4.22
Clinton Co.						

Figure 4.1 and Table 4.2 show that the overall best performer is an OGDC project (CSN19042B), and that three OGDC projects are performing poorly. A significant finding is that the 41 ft JRCP project, CSN19042 B, has not developed any distress after 10 years of service life, despite a large variation in OGDC layer thickness within the 500 ft. test section varying from 4in. in thickness of 5G crushed stone material to a 2in. thick 3G material and relatively poor particle size for acquiring stability. Particle size analysis of the OGDC material shows that the gradation falls substantially below the 0.45 power curve indicating possible lower stability. Section 19042 C, which is the adjoining east bound project, also classifies as an excellent performer given that it also consists of 41ft slabs and the transverse cracking is of low severity (i.e. without spalling) and small crack width. These cracks are most likely related to hot weather construction as discussed below, and have not had any detrimental effect on longer-term performance. For both these projects no measurable faulting was observed. The 19042 C job has a more uniform base layer thickness of 4 inches consisting of 3G crushed stone.

Figure 4.1 and Table 4.2 also show that OGDC projects 77023, Section A and 77024A, have the highest degree of transverse cracking, spalling and (faulting), and that these cracks over time have moved from low severity to the moderate severity category due to the associated spalling. For both these projects distress is moisture related as will be discussed in more detail in section 4.3.

The high degree of mid-slab cracking in JPCP for CSN 11017 Sections A and C EB, I-94, is of concern. Since, by definition, JPCP has no reinforcement, mid-slab transverse cracking may lead to premature loss of load transfer, faulting and spalling, all associated with crack opening. Close to one year after construction, approximately 30 percent of the panels EB for two of the three sections (A and B) developed mid-slab transverse cracks of which half are full width. The third section EB showed approximately 20 percent of the slabs had developed cracks and 6percent of slabs had full width cracks. Mid-slab transverse cracking was found to propagate from the outer edges inwards and coring verified that it was from the top downward without any signs of faulting or pumping. In addition, information on the PCC placement conditions reinforces the belief that this behavior is related to hot weather related construction problems. The WB section constructed early spring of 1996 show no such distress.

Cores from the site obtained at partial width cracks show that cracking originated from the top (wider) and had a depth of approximately 6 inches, which is half the slab thickness. This is seen in Figure 4.2. The crack depth is greater than would be expected from plastic and drying shrinkage effects alone. The observed top down cracking for this project eliminates attributing this cracking to loss of slab support associated with the

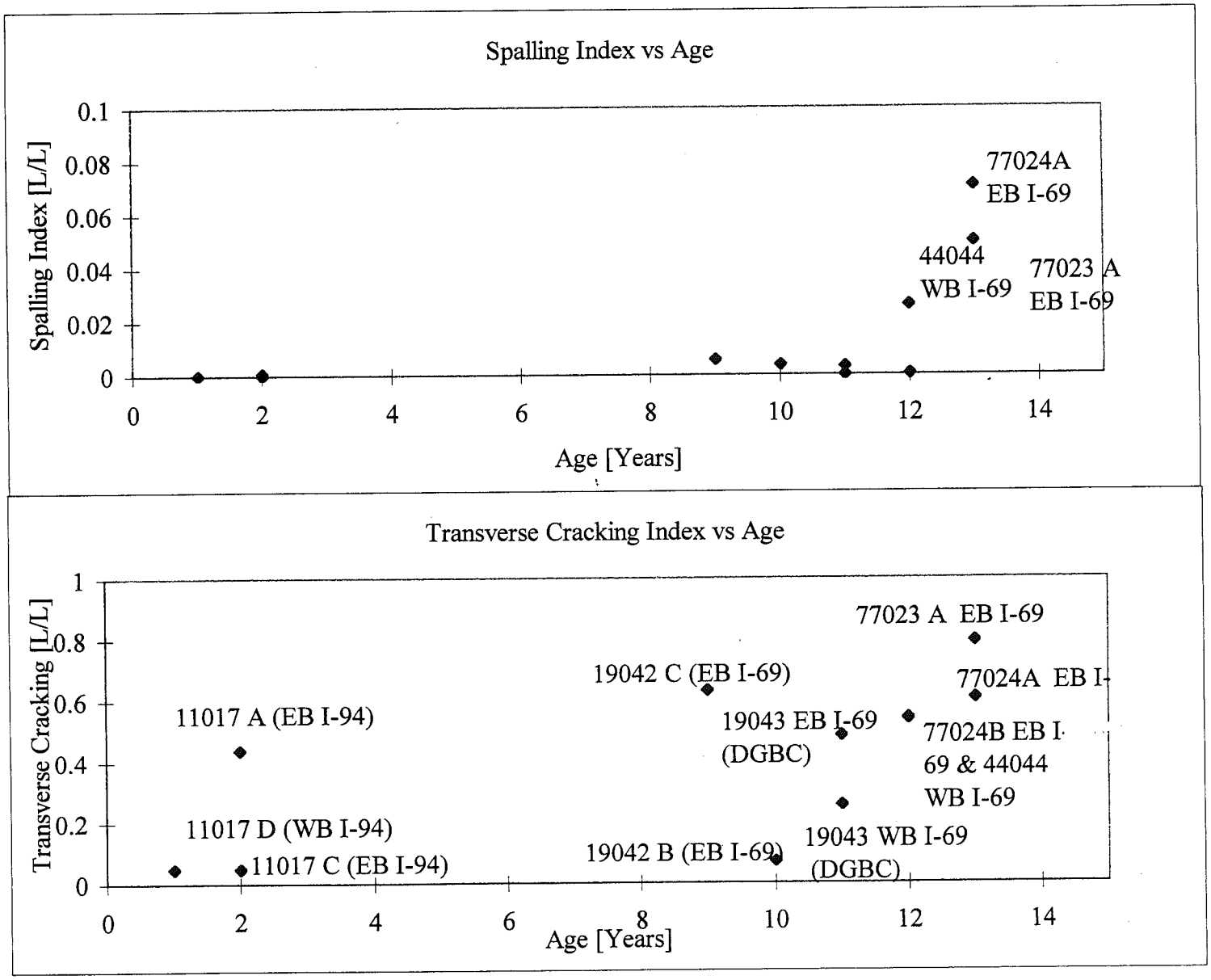

Figure 4.1 Normalized transverse cracking and cracking.

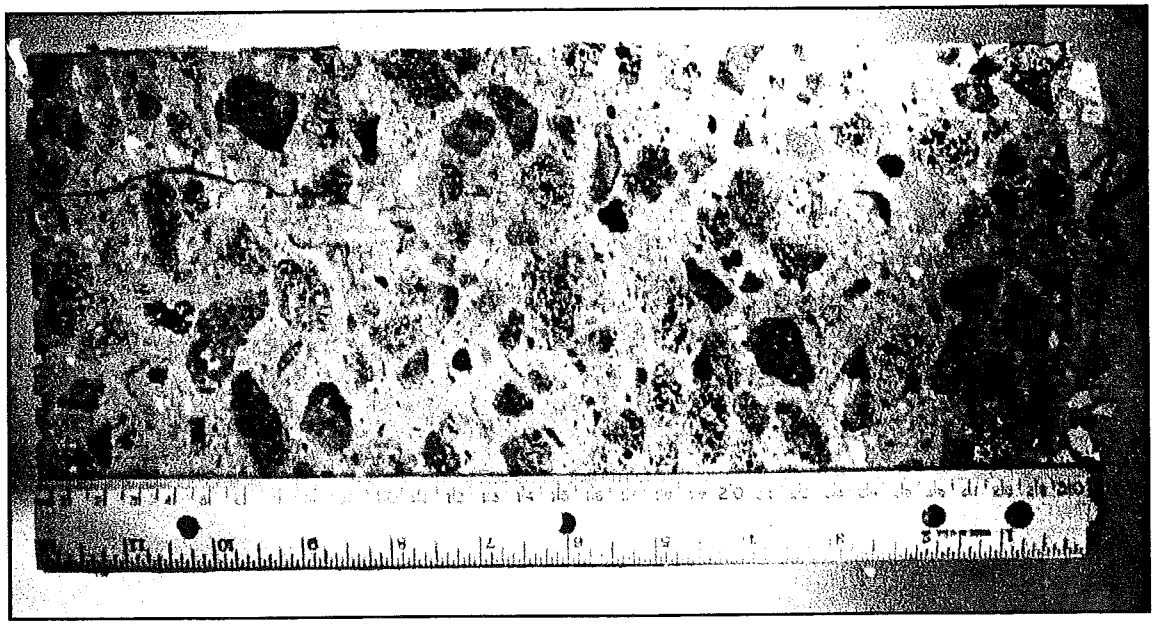

Figure 4.2 *Top-down cracking of CSN 1101734 Sec A on I-94, EB near Watervliet.*

OGDC layer. The origin of this type of distress is clearly temperature related as discussed in Section 4.3

The development of cracking and spalling in section A occurs at an unacceptable rate. During a revisit in November of 1997, six months after field testing, several (5) partial width cracks had propagated within the 500 ft. section to full width and full depth cracks, as verified from subsequent coring. The additional crack development is most likely due to rapid crack propagation through the weakened section.

4.3 Temperature Effects on Transverse Cracking

Test sections 19042 C and 11017 Section A stand out as having higher degree of low severity transverse cracking, as compared to their project counterparts (i.e. CSN 19042 B and CSN 11017, sections C and D, respectively). In both cases hot weather paving conditions occurred, and it is believed that this is the most plausible explanation why mid-slab cracking has occurred.

The most striking example of premature transverse cracking is the JPCP project on I-94, by Watervliet. High temperature placement of the short jointed plain slabs (15 and 16 ft) has resulted in a high frequency of full width midslab cracks. The WB job constructed the following year in cool spring weather does not have a single visible transverse crack. All other factors were constant (i.e. same contractor, base, subbase, PCC mix etc.). The only two known differences are: hot and sunny weather weather conditions, and bi-directional traffic occurred on the EB pavement sections with the early transverse cracking problems.

MDOT historical records show that concrete placement temperatures for the EB sections A-C were averaging 83 °F combined with hot sunny weather conditions. The MDOT construction report by Mr. Anderson and Mr. Miller document this. Hairline cracking in the mainline slab was observed by the MDOT resident engineer within the first day of pavement construction for the EB job in the area between stations 1881-1883. From station 1893+00 to 1881+00 there are several areas of full slab length longitudinal cracks requiring repair by means of cross-stitching. Later it was noticed that mid-slab transverse cracks were developing in the same area. In mid September, about one week after completing the EB sections A-C nighttime lows in the high 40's °F were reported. Thus the restrained slab contraction due to thermal effects is in the range of 80-100 °F within the first 28 days of the life of the concrete. This "thermal load" is substantial.

The difference in placement temperatures for summertime conditions for the EB direction and early spring conditions for WB are clearly demonstrated and are shown in Appendix E. The MDOT construction records listing the PCC placement temperatures and air temperatures, where available, were used to construct these curves. WB section D, which has no transverse cracking after about 1.5 years in service, was paved in early spring of 1996 during which time the PCC placement temperature averaged 68 °F. Although no air temperature data is available the combined effect of lower ambient temperature and initial PCC temperature is substantial, and most certainly result in considerable reduced internal tensile stresses in the hardening concrete due to much smaller thermal contraction and construction curling.

The distress surveys presented in Appendix C show that transverse cracking in OGDC pavements is present in most cases, except when the PCC placement temperatures are below about 70 °F. Typically, this is the case in Michigan during early spring (i.e. April/May) or late fall (October/November). The best OGDC performers all have lower temperature placement condition in common. Thus it is plausible that higher placing temperatures increase the amount of transverse cracking in JRCP and JPCP. This condition however does not necessarily lead to premature faulting and spalling in JRCP (i.e. CSN 19042 B and C).

Temperature effects can also explain the large amount of low severity transverse cracks found in the 41 ft JRCP (CSN 19042 C) on EB I-69. Virtually no cracking has occurred in section 19042 B. The average concrete placement temperature was 65°F. The average air temperature at time of PCC placement was 59 °F. This is consistent with a smaller slab contraction early in the life of a pavement. Consequently, the slab is mostly in the state of internal compression due to restraint expansion from joint and base friction, whereas section C is mostly in tension, except when slab cracking has occurred.

4.4 Moisture Effects on Distress

It is believed that the widened cracks in section 77023A and 77024A, which have spalled and faulted, are primarily the result of trapped water in the subbase (i.e. areas of least drainage), leading to loss of support within the OGDC layer.

It was observed that the drain outlets in the two sections were clogged. The cause of the clogging could not be determined, but it may have occurred as part of construction or after the pavement entered service. The fact that these outlets are clogged indicates that free water cannot be drained from beneath the pavement structure, thus leading to

saturated conditions. Presence of free water was verified through visual observation at the subbase/subgrade interface during boring in section 77024A.

This visual information is backed up by dynamic cone penetration (DCP) results shown in Appendix I . DCP penetration values are higher for the 77023 and 77024A projects for both the base and subbase indicating loss in strength and confinement.

Resilient modulus testing by the research team (see Appendix K) showed a significant reduction in base course resilient modulus when tested in an undrained condition (i.e. saturated). This loss of strength/stiffness is associated with the occurrence of high permanent deformation and this effect would be expected to be more severe in supporting layers composed of rounded aggregate particles, such as that found for the 77024A project.

Table 4.3 summarizes the mean and standard deviation values for resilient modulus for the different OGDC (3G, 350 AA) and DGBC (21AA) materials and moisture conditions. Appendix K presents the detailed results of this analysis. As expected resilent modulus decreases sharply under saturated moisture conditions for all gradations tested. Thus if clogging of the drain outlets occur and undrained or saturated condition exists, dramatic reductions in the layer stiffness would result. This loss of support, when it prevails, is the most plausible explanation for the accelerated deterioration of the OGDC projects 77023A and 77024A. These projects had a pronounced deterioration in the truck lane only, indicating that the primary distress mechanisms are associated with truck traffic load.

Table 4.3 Summary of resilient modulus testing.

Aggregate Type	Gradation	Moisture Condition	Mean M_R (MPa)	Standard deviation
Glacially	**21AA**	Dry	431.3	23.9
Derived		Drained	414.6	39.9
		Undrained	139.6	11.7
	350AA	Dry	416.3	5.32
		Drained	369.8	30.3
		Undrained	153.5*	39.2*
	3G	Dry	389.7	29.0
		Drained	375.4	21.5
		Undrained	187.4*	60.0*
Quarried	**21AA**	Dry	431.5	24.4
Limestone		Drained	350.1	22.6
		Undrained	108**	**
	350AA	Dry	349.3	11.4
		Drained	313.7	13.9
		Undrained	***	***
	3G	Dry	368.5	18.6
		Drained	327.4	18.9
		Undrained	129.3	39.7

Note: The * symbol indicates that 2 of the samples made it to step 11 before softening. ** Indicates 1 sample lasted until step 11. *** Indicates that no samples made it to step 11.

In the case of the poor performing sections evaluated in this study, high levels of faulting (approximately 0.25 to 1 inch (6 to 25 mm)) and severe spalling (due to high differential vertical deflections under truck loading) have been observed. In contrast to the poor performance of the above-mentioned project (77024-20821A), another I-69 pavement section in St. Clair County has performed well under similar traffic and environmental conditions. The better performing 77024-17988A was constructed of similar slab thickness in the same year (1984) on crushed gravel OGDC base material separated from the subgrade by a 18 inch clean sand subbase. The subgrade has a 56 percent silt and clay content.

It was observed that the drain outlets for this section were clear, and there is little evidence of loss of slab support. The unclogged drain outlets expedite the drainage of free water from the pavement structure and the thick subbase would help prevent the intrusion of fines from the subgrade into the drainable base while offering additional

support both during construction and while in-service. The use of a crushed aggregate OGDC would offer additional shear strength. In combination, these factors greatly reduce the potential for pumping through the minimization of free water in the pavement structure and increased support.

Table 4.4 lists the averaged filter criteria values calculated from sieve analysis results for the base, subbase and subgrade for all the sections. Overall, the values are within limits suggested by FHWA. The table also illustrates that permeability of OGDC systems should be higher than that of the DGBC as indicated by the higher ratios of D15(base)/D50(subbase). Thus, if properly drained (i.e. connected to an operational sub-drainage system), the use of an OGDC will lead to improved drainage directly beneath the slab and a reduction in distress associated with presence of free water. It is for this reason that there has been a national commitment to the use of OGDC over DGBC in recent years.

The open structure of the OGDC allows for the relatively rapid movement of water, exposing the sub-base surface to higher water velocities during and immediately following precipitation events. This can lead to erosion of the subbase material and clogging of the drainage system. Because of these erosion concerns, the same sub-base gradation that is compatible with dense graded base courses may be incompatible with an OGDC layer. Of great importance is the amount of fine material (passing the No. 200 sieve) in the sub-base used with an OGDC system.

This is supported by test section 77023-21586A, where the sub-base was found to contain 15 percent fines (silt and clay) passing the No. 200 sieve. The origin of these fines is uncertain, but they may have either been constructed into this layer through poor gradation control or possibly migrated upward from the subgrade under the action of traffic. It is likely that these fines are responsible for the clogging of the subdrains noted previously. As discussed, once the drainage system became clogged, the base layer remained in an undrained condition for prolonged periods of time after a precipitation event. This would lead to a dramatic reduction in the resilient modulus of the supporting materials and an increase in the permanent deformation compared to materials in a drained condition. This in turn can lead to permanent settlement of the slab, erosion of subbase, faulting and further clogging of drainage structures. Had this subbase been used under a dense graded base, these fines likely would not have eroded into the drainage system.

Table 4.4 FHWA filter criteria calculations based on laboratory sieve analysis results.

Projects	Uniformity (D60/D10)		% Passing #200		Infiltration D15(filter)/D85(soil) <=5	<=5	Compatibility D50(filter)/D50(Soil) <=25	<=25	Drainage D15(Filter)/D15(Soil) >=5	>=5
	Base	Subbase	Subbase	Subgrade	Base/Subbase	Subbase/Subgrade	Base/Subbase	Subbase/Subgrade	Base/Subbase	Subbase/Subgrade
OGDC										
77023-21586A	3.7	3.7	15.1	54.1	11.6	0.3	40.4	2.5	46.7	
77024(A)-20821A	11.6	21.3	4.6	76.2	0.5	1.8	5.6		23.5	
77024(B)-17988A	3.7	2.8	10.2	59.7	16.6	0.4	49.9	0.6	41.7	
19042-24680A Sec B	8.0	3.3	6.9	10.3	10.9	0.2	37.9	0.9	48.7	
19042-02233A Sec C	10.3	3.3	6.3	14.7	2.0	0.2	43.3	1.3	15.3	
44044-18804A	30.3	5.6	8.4	18.1	0.5	30.7	0.0	1.1	26.1	1.0
11017-32516A Sec A	2.2	3.8	6.7	na	7.7		30.1			
11017-32516A Sec C	2.4	2.1	11.3	na	18.1		48.9			
11017-32516A Sec D	1.6	3.4	6.7	na	11.1	0.4	32.6	2.2	44.5	2.3
DGBC										
25132-06582A	32.1	4.7	8.1	50.8	0.2	0.3	6.9	2.1	1.2	
19043-02234A WB	26.6	3.0	10.0	11.2	0.5		9.2			1.9
19043-02234A EB	25.9	3.9	9.7	na	0.2	0.1	7.9	1.1	1.7	1.0

In another section, 77024(A)-20821, the silt and clay content of the subbase is within the specified limits. Yet, trapped water was observed in the lower part of the subbase. In this case, the reasons are clogged drains combined with silt and clay of 76 percent in the subgrade. It appears that fines were eroded and pumped from the subgrade into the drainage system. Three other sections were also found to have high silt and clay content in the subgrade. They are the 77024(B)-17988, 77023-21586 and 25132-06582 The only one exhibiting good performance was 77024(B). It is believed that the very thick 18-inch subbase protected the system from erosion of subgrade fines.

It is noted that the best performing OGDC sections (19042B-24680A, 77024-17988A, 19042C-02233A) all deviate, at least to some degree, from the established filter criteria between the OGDC base and subbase. However, these sections have a thick sand embankment or sand subbase separating the OGDC from the subgrade. This again supports the contention that increased layer thickness above fine-grained subgrade soils will help ensure that adequate support during construction and service is provided while preventing the intrusion of subgrade materials into the OGDC drainage system. This is also believed to be valid for the DGBC sections 19043-02234A westbound and eastbound.

For the Watervliet sections, the potential infiltration of fines from the subbase into the base has been mitigated by using a geotextile separator. Inadequate filter values between the base and subbase have been addressed since 1989 through the use of a separator layer (either aggregate or geotextile). Nonetheless, attention should still be given to proper handling of fine materials, particular where high fines in subgrades are present.

Most likely reasons for the excellent performance of CSN 19042 B are: low temperature PCC placement temperature (68 °F), the low P200 in the subbase (7.5 percent), thickened subbase (i.e. > 8 inches) and sandy subgrade. This would result in a well drained pavement. Field observations showed that the drains were partly clogged, which will pose a problem if not maintained. Expansion joints were found every 328ft. One would expect that the restrained tensile stresses in the slab from early age heating and cooling are insignificant, and trapping water in the subbase should not be a problem due to low fines in the subbase and the subgrade.

4.5 PCC Mechanical Properties Effect On Transverse Cracking

The pavement sections evaluated under this study did not show any strength-dependent performance trends as the compressive strength values are substantially above the required minimum strength of 3,500 psi. This is seen from the extensive test results shown in Tables 4.5 and 4.6. In table 4.5 the field compressive strength and elastic modulus values are shown together with average and standard deviation values. The average field compressive strength for the older sections (i.e. without the 11017) was 6,619 psi with a low of 5,670 psi (CSN 25132) and a high of 7,450 psi (CSN 44044). CSN 11017 sections A and C, EB, had a two-year average compressive strength of 6,775 psi versus 5,690 psi for section D, WB, which had no distress. The individual test results for the field core tensile strengths together with average and standard deviation are shown in Table 4.6 for all sections tested.

Table 4.5: Measured compressive strength and elastic modulus of field cores.

Test Section	Cylinder ID#	Station Location	Specimen Length (in)	Specimen Diameter (in)	L/D Ratio	L/D Correction Factor	Ultimate Load (kips)	Compressive Strength (psi)	Corrected Compressive Strength (psi)	Elastic Modulus (psi)
11017-32516A EB Section A	M2	1790+49	11.5	5.9	1.95	0.99	176.7	6200	6140	4.52E+06
	M4	1793+52	11.5	5.9	1.95	0.99	186.6	6600	6530	4.63E+06
	M6	1794+83	11.75	5.9	1.99	1	195.1	6900	6900	4.77E+06
	Average								**6520**	**4.64E+06**
	Std								**380**	**1.25E+05**
11017-32516A EB Section C	M2	1683+48	11.5	5.9	1.95	0.99	197.9	7239	7170	4.08E+06
	M3	1684+35	11.5	5.9	1.95	0.99	185.2	6774	6710	4.51E+06
	M5	1687+01	11	5.9	1.86	0.985	206.5	7315	7210	
	Average								**7030**	**4.30E+06**
	Std								**278**	**3.04E+05**
11017-32516A WB Section D	M1	1783+39	11.25	5.9	1.91	0.99	154.1	5640	5580	4.12E+06
	M7	1788+11	11.75	5.9	1.99	1	155.6	5694	5690	4.02E+06
	M13	1784+98	11.75	5.9	1.99	1	158.4	5795	5800	6.37E+06
	Average								**5690**	**4.84E+06**
	Std								**110**	**1.33E+06**
19042-24680A EB Section B	6M	279+10	9.5	6	1.58	0.97	157.6	5574	5410	4.10E+06
	8M	279+87	9.6	6	1.60	0.97	201.2	7116	6900	4.68E+06
	9M	280+30	9.6	6	1.60	0.97	197.5	6985	6780	5.01E+06
	Average								**6360**	**4.60E+06**
	Std								**828**	**4.61E+05**
19042-02233A EB Section C	1M	527+68	8.9	6.1	1.46	0.95	195.6	6693	6360	4.62E+06
	9M	530+95	9	6	1.50	0.96057348	197.2	6975	6700	4.59E+06
	11M	531+23	9.2	6.1	1.51	0.96	205.1	7018	6740	4.98E+06
	Average								**6600**	**4.73E+06**
	Std								**209**	**2.17E+05**
19043-02234A EB	3M	137+42	8.8	6	1.47	0.95	234.9	8308	7890	4.98E+06
	7M	138+26	8.8	6	1.47	0.95	203.1	7183	6820	4.58E+06
	10M	138+62	8.9	6	1.48	0.96	194.6	6883	6610	6.12E+06
	Average								**7110**	**5.23E+06**
	Std								**686**	**7.99E+05**
19043-02234A WB	1M	149+68	8.2	6.1	1.34	0.95	224	7665	7280	6.00E+06
	8M	148+60	8.25	6.125	1.35	0.95	214.9	7353	6990	5.71E+06
	13M	147+85	8.2	6.1	1.34	0.95	180.8	6187	5880	4.77E+06
	Average								**6720**	**5.49E+06**
	Std								**739**	**6.43E+05**
25132-06582A SB	M1	660+19	8	5.9	1.36	0.955	169.7	6207	5930	5.66E+06
	M2	659+19	8.5	5.9	1.44	0.96	138.5	5068	4870	5.83E+06
	M4	655+56	8.75	5.9	1.48	0.97	175.3	6413	6220	5.57E+06
	Average								**5670**	**5.69E+06**
	Std								**711**	**1.30E+05**
44044-18804A WB	3M	671+01	8.9	6.1	1.46	0.95	257.8	8821	8380	5.10E+06
	7M	669+35	9.1	6.125	1.49	0.96	196.1	6710	6440	4.04E+06
	9M	668+56	9	6	1.50	0.96	221.8	7845	7530	5.01E+06
	Average								**7450**	**4.72E+06**
	Std								**972**	**5.88E+05**
47065-28215A EB	C3	700+00	10	5.9	1.69	0.98	139.9	4951	4850	3.65E+06
	C5	I-96 Bus.Lp	10.75	5.9	1.82	0.985	123	4851	4780	3.36E+06
	C7	810+63	10.25	6	1.71	0.98	137.1	4351	4260	3.61E+06
	Average								**4630**	**3.54E+06**
	Std								**322**	**1.54E+05**
47065-28215A WB	107		9.5	5.9	1.61	0.97	125.83	4605	4470	3.79E+06
	113		10	5.9	1.69	0.98	100.39	3674	3580	3.00E+06
	122		10	5.9	1.69	0.98	141.4	5175	5050	3.74E+06
	Average								**4370**	**3.51E+06**
	Std								**740**	**4.42E+05**
77023-21586A EB	M1	1820+74	9	5.9	1.53	0.97	197.9	7239	7020	5.69E+06
	M8	1827+70	9.25	5.9	1.57	0.98	207.8	7602	7450	5.22E+06
	M10	1827+97	8.75	5.9	1.48	0.97	189.4	6930	6720	5.11E+06
	Average								**7060**	**5.34E+06**
	Std								**367**	**3.12E+05**
77024-20821A EB Section A	M0	83+64	9.1	6	1.52	0.96	199.5	7056	6770	5.49E+06
	M6	88+58	9	6	1.50	0.96	191.7	6780	6510	5.37E+06
	M10	89+64	9.05	6	1.51	0.96	195.3	6907	6630	6.03E+06
	Average								**6640**	**5.63E+06**
	Std								**130**	**3.52E+05**
77024-17988A EB Section B	1M	408+14	9.1	6.1	1.49	0.96	196.5	6724	6460	4.34E+06
	6M	414+67	9.56	6.125	1.56	0.97	166.7	5658	5490	4.30E+06
	9M	416+18	8.8	6	1.47	0.96	174.4	6168	5920	4.74E+06
	Average								**5960**	**4.46E+06**
	Std								**486**	**2.43E+05**

Table 4.6 Tensile strength (split cylinder) of field cores

Test Section	Cylinder ID.	Station Location	Specimen Length (in)	Specimen Diameter (in)	Ultimate Load (kips)	Split Tensile Strength (psi)
11017-32516A EB Section A	M1	1790+17	12	5.9	65.61	635
	M3	1790+80	11	5.9	68.6	655
	M5	1794+53	11	5.9	64.43	635
	Average					**640**
	Std					**12**
11017-32516A EB Section C	M1	1682+90	11.25	5.9	67	645
	M4	1685+41	11	5.9	59.02	580
	M6	1689+10	11	5.9	56.02	525
	Average					**585**
	Std					**60**
11017-32516A WB Section D	M5	1786+53	11	5.9	57.03	560
	49	1789+70	11.25	5.9	60.02	575
	M11	1791+27	11.75	5.9	58.02	535
	Average					**550**
	Std					**20**
19042-24680A EB Section B	2M	276+59	8.2	5.9	48.89	645
	4M	277+82	8.8	5.9	48.52	595
	10M	280+71	9.4	5.9	49.3	565
	Average					**600**
	Std					**40**
19042-02233A EB Section C	3M	527+96	8.5	5.9	51.56	655
	6M	528+93	8.4	5.9	55.67	715
	7M	529+14	8.4	5.9	47.7	615
	Average					**660**
	Std					**51**
19043-02234A EB	6M	137+91.5	8.8	5.8	38.36	480
	12M	138+75.5	8.5	5.9	45.99	585
	13M	138+82.5	8.9	6	49.2	580
	Average					**550**
	Std					**59**
19043-02234A WB	4M	149+17.6	7.8	5.9	42.89	595
	6M	148+68.7	8.3	5.9	43.12	560
	10M	148+22.4	8.1	5.9	46.18	615
	Average					**590**
	Std					**28**
25132-06582A SB	M3	657+20	8	5.9	53.03	720
	M5	653+71	8.625	5.9	55.5	695
	M7	650+10	9.125	5.9	52.5	620
	Average					**680**
	Std					**52**
44044-18804A WB	2M	671+21	8.8	6	46.08	555
	12M	666+92	9.1	5.9	44.23	525
	13M	666+23	8.6	5.8	45.32	580
	Average					**555**
	Std					**28**
47065-28215A EB	C2	670+00	9.25	6	47.5	545
	C4	720+00	10.5	6	59.5	600
	C6	788+24	10.5	6	62.5	630
	Average					**590**
	Std					**43**
47065-28215A WB	110		9.5	5.9	41.03	490
	116		10	5.9	53.99	570
	118		10	5.9	60.55	655
	Average					**570**
	Std					**83**
77023-21586A EB	M4	1822+93	8.75	5.9	55.5	685
	M7	1825+10	9	5.9	60	720
	M14	1834+50	9	5.9	63	770
	Average					**725**
	Std					**43**
77024-20821A Section A	M3	85+43	8.6	5.9	52.1	655
	M4	87+05	8.8	5.9	61.72	755
	M7	88+85	9	5.9	63.09	755
	Average					**720**
	Std					**58**
77024-17988A Section B	3M	409+47	8.9	5.9	53.25	645
	8M	415+93	8.65	5.9	49.62	620
	13M	418+17	8.7	5.9	45.7	565
	Average					**610**
	Std					**41**

4.6 Load Transfer Evaluation of Cracks and Joints Using FWD

4.6.1 Effect of Coarse Aggregate Type

Good load transfer will help reduce pavement distresses such as faulting, pumping, loss of support, transverse cracking, corner breaking, and spalling. Commonly, the load transfer behavior of concrete pavements is described by the deflection based load transfer efficiency, LTE, which is defined as the relative deflection between two adjacent slab edges when one slab is loaded. Figure 3.6 (p.21) shows the FWD Kuab sensor location. Generally, it is desirable to maintain deflection LTE above 70 percent to ensure good long-term performance.

Load transfer was measured for both approach and leave slabs. Table 4.7 presents the calculated values. All test sections under JRCP, with gravel or limestone as PCC coarse aggregate, show high and sufficient load transfer at both the approach and leave slabs, ranging from 75 to 100 percent. This indicates that evaluated DGBC and OGBC sections both have good load transfer with no apparent effect of base type for the different concrete types. On the other hand, the slag concrete pavement at Watervliet shows systematically lower load transfer for the approach joint/crack compared the leave joint/crack. This is seen from Table 4.8. The load transfer is on the order of 35 percent for the approach, and 70 percent for the leave.

Table 4.8 also illustrates that spring construction produces higher initial joint load transfer (nearly 100 percent), whereas summer construction typically has initial joint load transfer of about 75 percent and up. This is expected as summertime construction result in larger crack width and consequently lower initial LTE values. Thus initial LTE values in Michigan at joints fall in the range of about 80% to 100% irrespective of the coarse aggregate used in the PCC slab.

This study has found no performance problems associated with joints. All the joints look like they are functioning well and thus no joint design changes are recommended.

The consistently lower LTE for the slag concrete, as seen from Table 4.8, used for project 11017 can not be ignored. Further evaluation shows that the deflections of the loaded slab on approach joint/crack is greater by 2-6 mils. This indicates that the support is reduced probably due to void formation under the loaded slab, which is more pronounced during morning-hour conditions.

the approach slab. Particle size analysis of the 3G OGDC material used for the JPCP project shows that the gradation falls substantially below the 0.45 power curve indicating possible lower stability, which may become a factor when aggregate confinement is reduced such as underneath a cracked slab (i.e. joints and mid-slab cracks).

Table 4.7 Typical LTE values for joints & cracks from FWD results.

Test Section	Route	Year Open	Date & Year Tested	FWD test	Joint or Crack Load Transfer Efficiency Approach %	Leave %	Ave. Crack Width mils
19042 B-24680	I-69 EB	1986	8/14/96				
				Joint	82	85	
				Crack	100	NA	6
				Crack	98	NA	3
				Crack	96	NA	12
19042 C-02233A	I-69 EB	1987	8/7/96				
				Joint	98	99	
				Crack	93	84	16
				Crack	96	83	16
				Crack	101	79	2[illegible]
				Crack	NA	74	31
				Crack	23	81	24
19043-02234A Dense Graded Base Course	I-69 EB	1981	8/15/96				
				Joint	86	94	
				Crack	103	85	20
				Crack	NA	102	20
				Crack	98	80	24
				Crack	102	86	24
				Crack	102	81	24
				Crack	99	NA	12
				Crack	99	80	24
				Crack	98	NA	12
				Crack	99	86	20
				Crack	97	NA	4
				Crack	92	87	20
19043-02234A Dense Graded Base Course	I-69 WB	1981	10/2/96	Joint	74	82	
				Crack	99	96	10
				Crack	95	99	13
				Crack	95	96	10
25132-20821 Dense Graded Base Course	I-475 SB	1981	6/26/97	Joint	77	77	
44044-18804A	I-69 WB	1984	7/23/96	Joint	95	92	
				Crack	97	NA	24
				Crack	51	NA	31
77023-21586A	I-69 EB	1984	7/2/97	Joint	92	97	
				Crack	72	105	20
				Crack	52	82	12
				Crack	91	92	12
				Crack	17	13	24
				Crack	30	95	20
				Crack	20	15	24
77024 A-17988	I-69 EB	1983	10/17/96				
				Joint	85	76	
				Crack	8	8	39
				Crack	98	99	24
				Crack	7	6	39
				Crack	9	7	39
				Crack	101	85	24
				Crack	19	26	39
77024 B-17988	I-69	1984	10/29/96				
				Joint	NA	80	
				Crack	98	89	12
				Crack	104	95	16
				Crack	101	94	13
				Crack	95	95	10

Table 4.8 Typical LTE values for joints & cracks from FWD results for the two year old JPCP sections on I-94 near Watervliet and a newly constructed pavement on I-96 near Howell before opening to traffic.

Test Section	Route	Station Location of Joint or Crack	FWD location	Ave. Crack Width mils	LTE Approach %	LTE Leave %
11017-32516	I-94 EB	1790+57	Joint		NA	70
Section C		1790+73	Joint		43	NA
		1791+06	Joint		NA	63
		1791+22	Joint		31	
		1794+12	Joint			57
		1794+28	Joint		51	
		1791+15	Crack 1	20	27	47
		1791+47	Crack 2	20	47	81
		1791+65	Crack 3	20	34	41
		1791+79	Crack 4	20	33	32
		1792+11	Crack 5	13	40	40
		1792+27	Crack 6	16	22	67
		1792+43	Crack 7	20	65	59
		1792+60	Crack 8	13	43	63
		1793+24	Crack 9	13	77	84
11017-32516	I-94 EB					
Section C		1682+62	Joint		26	81
		1682+78	Joint		26	83
		1686+62	Joint		37	78
		1689+99	Joint		38	72
11017-32516	I-94 WB					
Section D		1792+46	Joint		62	90
		1792+30	Joint		46	91
		1789+14	Joint		27	84
		1782+98	Joint		44	87

Before Traffic-1997:

					LTE%	LTE%
47065-28215A	I-96 WB					
	Base Type				Approach Joint	Leave Joint
	Limestone 350 A	typical	Joint		89	94
	Slag 350 AA	typical	Joint		99	97
	3G	typical	Joint		96	93

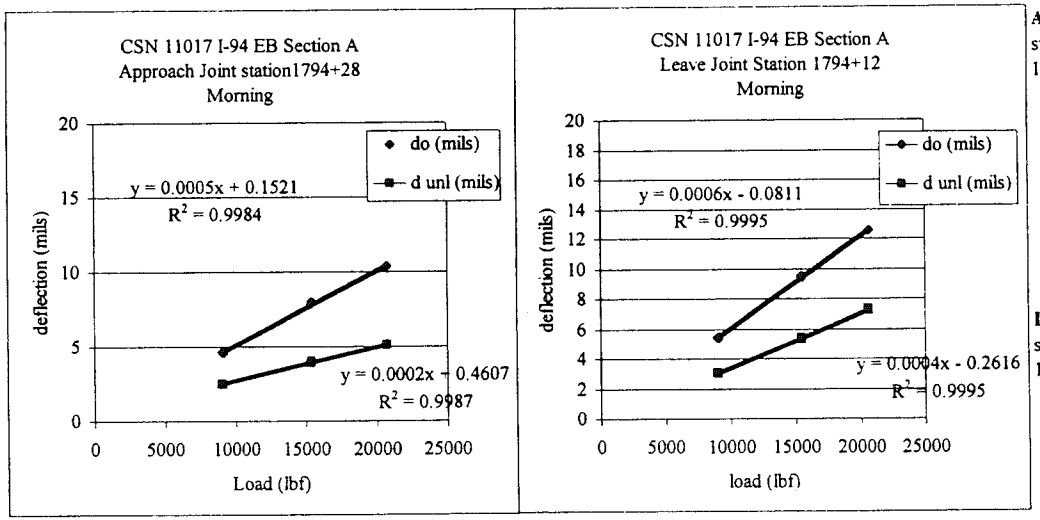

Approac Joint 11

station	load (lbf	do (mils)	d unl (mi	LTE (%
1794+28	9096	4.56	2.47	54
	9047	4.56	2.51	55
	9018	4.63	2.44	53
	15402	7.99	3.99	50
	15423	7.88	3.96	50
	15365	7.82	3.89	50
	20718	10.35	5.08	49
	20689	10.35	5.06	49
	20739	10.35	5.11	49

Leave Joint 8

station	load (lbf	do (mils)	d unl (mi	LTE (%)
1794+12	9047	5.46	3.04	56
	9047	5.39	3.02	56
	8989	5.42	3.04	56
	15464	9.5	5.38	57
	15423	9.5	5.41	57
	15473	9.41	5.3	56
	20624	12.51	7.3	58
	20606	12.51	7.26	58
	20651	12.57	7.23	58

Morning End Station

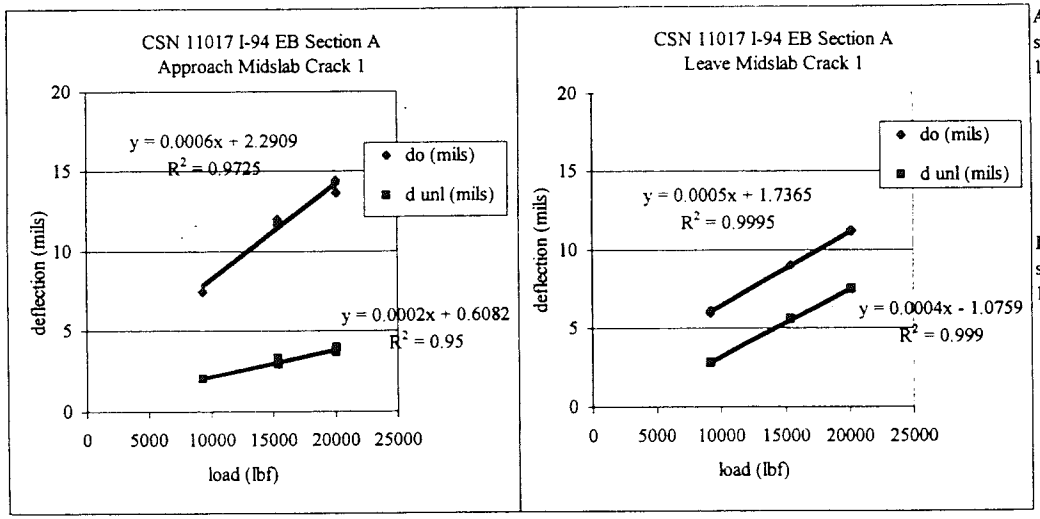

Approach Midslab Crack 12 inch from do

station	load (lbf	do (mils)	d unl (mi	LTE (%
1791+15	9313	7.44	2.05	28
	15395	11.61	3.04	26
	15464	11.78	2.96	25
	15381	11.97	3.33	28
	20081	14.37	3.75	26
	20101	13.63	3.96	29
	20059	14.26	3.69	26

Leave Midslab Crack 1 12 inch from do

station	load (lbf	do (mils)	d unl (mi	LTE (%
1791+15	9176	5.93	2.81	47
	9182	6.1	2.81	46
	9233	6.1	2.83	46
	15409	8.98	5.61	62
	15415	9	5.57	62
	15409	8.98	5.54	62
	20113	11.21	7.41	66
	20146	11.15	7.52	67
	20213	11.19	7.52	67

Figure 4.3 Typical FWD joint and crack deflection results and LTE for JPCP project on I-94 near Watervliet for morning conditions

4.6.2 Slab Deflection and LTE versus Transverse Crack Width in the Outer Wheel Path

Load transfer and d0 deflection results for the outer wheel path for all the JRCP sections studied (i.e. without the JPCP sections on I-94) are shown in Figure 4.4 versus the associated average transverse crack widths, as measured on the surface. The FWD d0 results have been normalized to 9,000 lb. The FWD results were obtained on the approach and the leave side of a crack. In general, the load transfer remains high (80 to 100 percent) and only slightly decreasing with increasing surface crack widths smaller than about 23 mils (0.60 mm). However, for larger crack widths the load transfer decreases rapidly, and spalling occurs. This deterioration mechanism seems to be consistent with increased slab deflection underneath the load as seen from the d0 deflection versus crack width results. Overall, these results show that aggregate interlock and LTE in Michigan JRCP's is rapidly decreasing for crack widths greater than about 23 mils (0.60 mm).

Spalled transverse cracks were found for both OGDC and DGBC supported JRCP for similar crack widths, indicating that the crack properties are perhaps the most critical factor for good long-term performance.

4.6.3 Mid-Slab Deflections

A comparison of mid-slab deflections from FWD for noon measurements was conducted to determine if any significant differences exist between the pavements constructed on OGDC versus DGBC and to determine if the variation in deflection over the test section length is significant.

Figure 4.5 illustrates the average interior slab deflection immediate underneath the load and normalized to 9,000 lb. FWD loading.

No consistent differences were found in the d0 deflection values from FWD testing for slabs on OGDC and DGBC. The DGBC projects CSN 25132 and 19043 EB and WB have d0 deflection values between 3 mils and 4.25 mils. This is seen from Figure 4.5

Also, lack of uniformity in slab support is known to contribute to slab cracking, Darter et al. (1995). Figure 4.5 shows that, for each project, the variation in mid-slab deflection along a project length, is in most cases within 10% of the mean value for each site, indicating that uneven settlement along the project length leading to transverse cracking

is not a factor. Same conclusions can be drawn from dynamic cone penetrometer (DCP) results as seen in Appendix I.

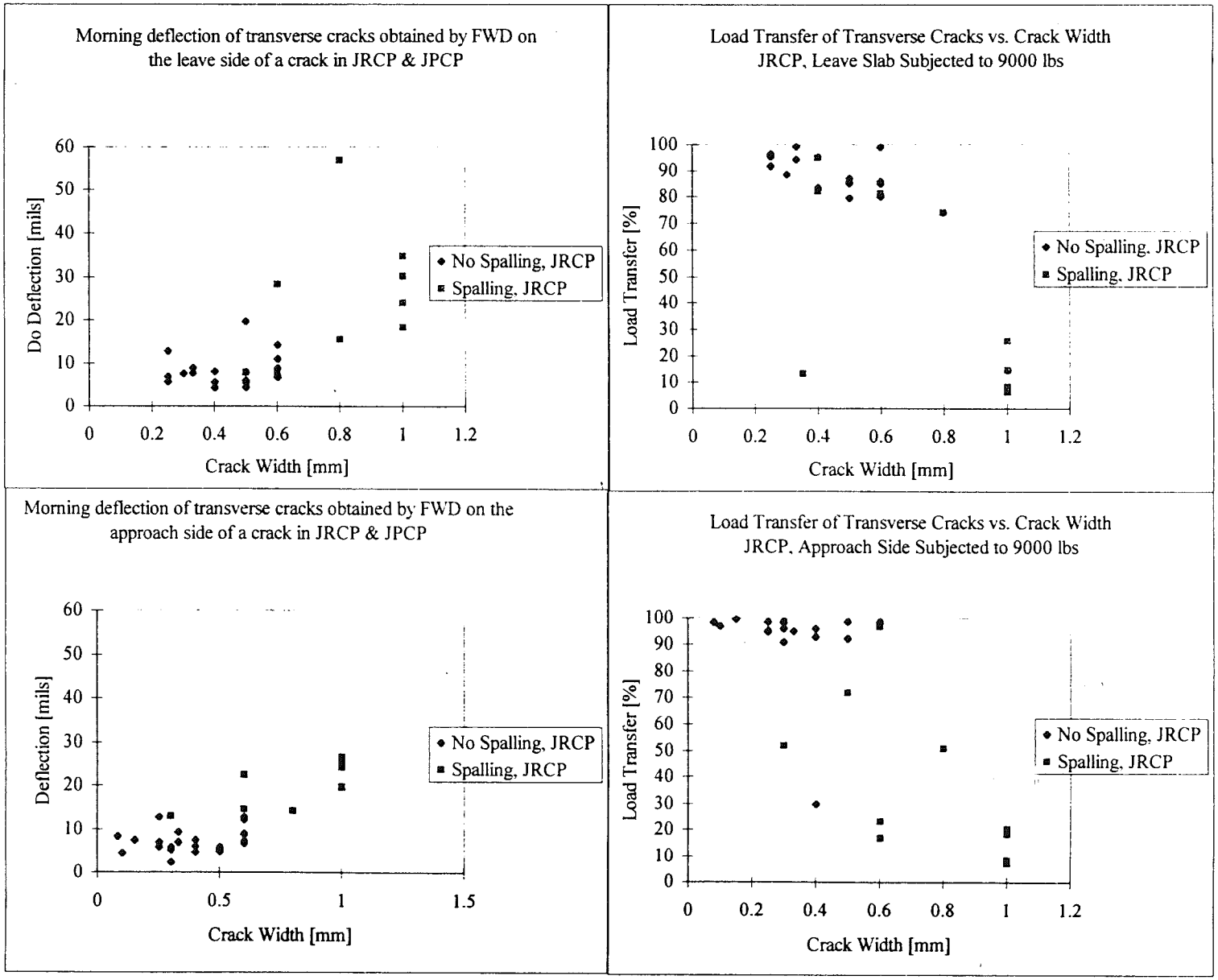

Figure 4.4 Slab deflection underneath the load and LTE values for 9000 lb FWD loading.

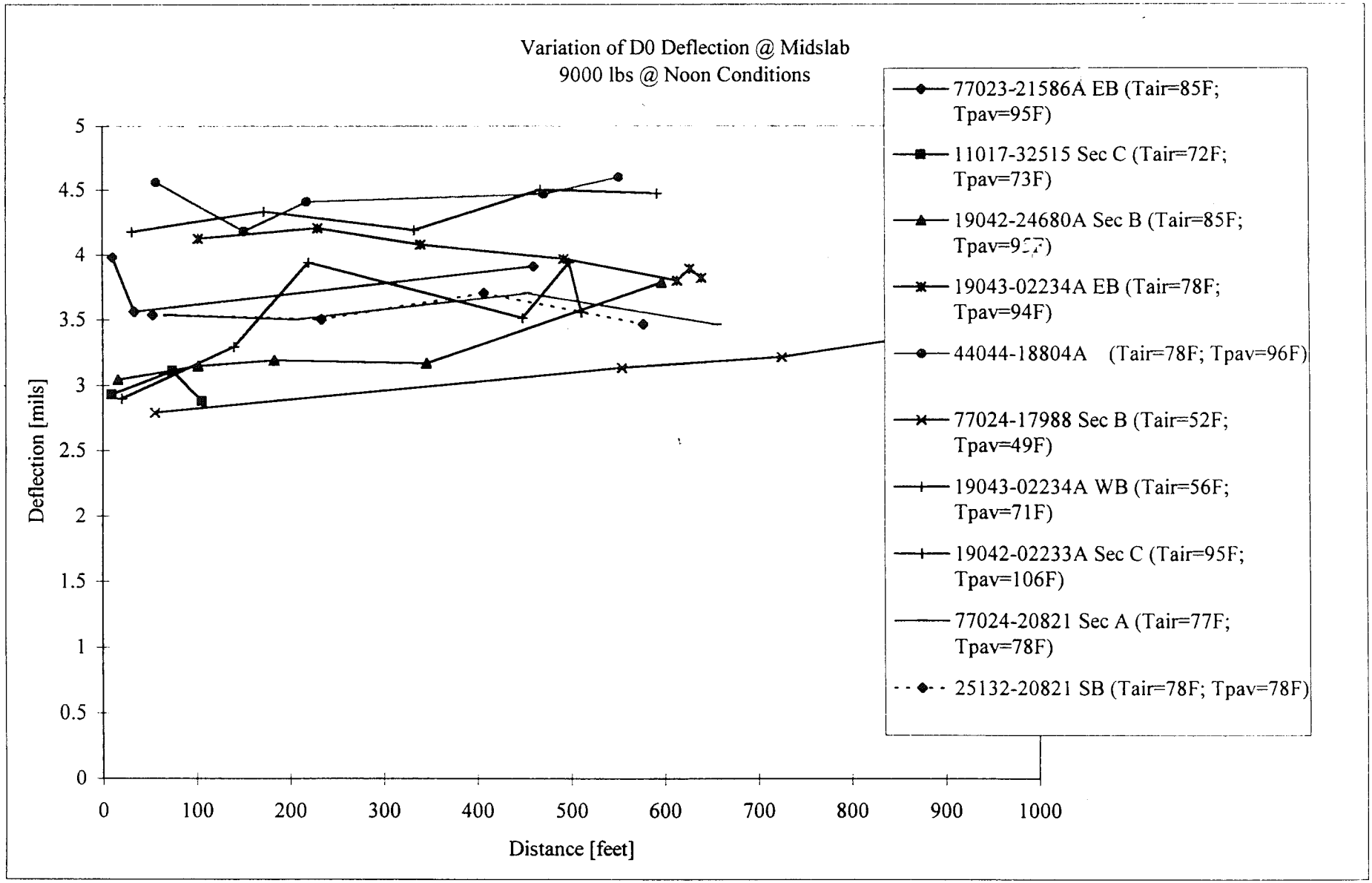

Figure 4.6 Slab deflection versus test length from FWD testing

5.0 CONCLUSIONS AND RECOMMENDATIONS

5.1 Conclusions

The following conclusions can be drawn based on a detailed field and laboratory investigation of 12 pavement sections in Michigan:

- Deterioration of OGDC pavements in terms of transverse cracking, spalling and faulting was found to be project specific and related to factors other than the OGDC itself. The major causes for accelerated deterioration were trapped water in the subbase causing loss of support and cracking, faulting and spalling under heavy traffic, and hot weather construction resulting in early cracking. This conclusion is based on a variety of measurements including MDOT PMS (distress points and RQI) data, visual drainage observations, distress measurements of transverse cracking, spalling, and faulting, MDOT historical records, soil sampling, and falling weight deflectometer testing.

- Premature mid-slab transverse cracking, for the 2-year-old JPCP project on I-94 CSN11017 sections A and C, EB, has developed from the top-down within the PCC slab consistent with high temperature construction and curing conditions. A field visit and coring conducted six months later found that some of these cracks had propagated into full-width, full-depth cracks. Traffic loadings likely helped the crack to propagate. Initial slab cracking is therefore not due to loss of support within the OGDC base. However, there are indications from FWD results that faulting is developing on the approach side of cracks and joints. This condition may result in premature faulting of cracks, increased slab stress under loading associated with higher deflections.

- One 10 year old, 41ft JRCP on an OGDC, CSN 19042B, has virtually no distress. Most likely reasons for the excellent performance are: cool springtime placement conditions with PCC average placement temperature of 68 F, low percent passing the No.200 sieve material in the subbase (7.5 percent), the use of a thickened subbase (i.e. > 8 inches), and sandy subgrade. Overall, these factors would result in a well-drained, well-supported pavement.

- Two OGDC pavements (CSN 77023 and 77024A) exhibited poor performance. Severely spalled and faulted cracks were present in the truck lane. Conditions leading to this include: clogged outlet drains, trapped water in the subbase/subgrade interface, associated loss of slab support, and high silt and clay content in the subgrade.

- MDOT historical records and distress measurements suggest that hot weather construction conditions (PCC placement temperatures approaching 90 °F on hot sunny days) are the most plausible cause of premature mid-slab transverse cracks. This is evident for projects 19042C and 11017 sections A-C. Cored field cylinders from these projects show that cracking has initiated on the slab surface. In the case of 19042C these cracks remained tight and have not affected long-term performance of the JRCP.

- Premature mid-slab transverse cracking can be minimized in JRCP and JPCP when construction conditions are consistent with cool weather conditions (i.e. low ambient temperature of less than 60 °F along with PCC placement temperatures below 70 °F). Two projects constructed under these conditions were found to be free of distress (CSN 11017 section D, and 19042B).

- For the JRCP's investigated in this study, FWD analysis show that crack widths greater than about 25 mils (0.6mm) have rapidly decreasing LTE and higher frequency of spalling. These results suggest that spalling of cracks may be associated with the increased deflection from heavy traffic loading. This finding may be useful to MDOT in evaluating a pavement condition based on average crack widths.

- This study has found no performance problems associated with joints. The joints are functioning well, and thus no joint design changes are recommended.

5.2 Recommendations as to Future Work and Methods to Improve Performance of the Next Generation of Concrete Pavements in Michigan.

The results from this study suggest that improvements in both construction and in the concrete mix can be made. Given that MDOT is moving towards JPCP as the standard pavement type, premature mid-slab cracking and spalling must be avoided.

The Role of Coarse Aggregate in Crack Resistance of JPCP's:

The Role of Coarse Aggregate in Crack Resistance of JPCP's:

- In view of the low load transfer at cracks and joints and the rapid development of spalling on the I-94 job (11017) near Watervliet, research is needed to investigate what can be done to optimize the PCC mix for JPCP to improve resistance to cracking in the first place and. Once cracking has occurred it should be investigated whether aggregate interlock can be improved for JPCP's on OGDC. The primary variables should be the coarse aggregate type and content, size, and gradation. Furthermore, the 11017 sec A concrete has shown rapid development of spalling. This may be either a mix or a construction related problem and needs to be investigated. Concurrent with this project MDOT initiated a second study entitled, "Transverse Crack Propagation of JPCP as Related to PCC Toughness", at the UM as part of the PRCE program.

- **Compatibility between PCC containing slag and OGDC type**
  Particle size analysis of the 3G OGDC material used for the JPCP project shows that the gradation falls substantially below the 0.45 power curve indicating possible lower stability, which may become a factor when aggregate confinement is reduced such as underneath a cracked slab (i.e. joints and mid-slab cracks). Compatibility between a PCC slab containing slag coarse aggregate and the OGDC should be further investigated.

Development of MDOT Database for Evaluating PCC Pavement Performance over Time:

- The distress development of JRCP and JPCP on OGDC should be quantified in terms of the individual distress types quantified (i.e. normalized transverse cracking and spalling, and faulting, versus age). See Section 4.2 for more detail. This will provide a strong database for developing performance-based specifications needed for optimizing pavement types (JRCP versus JPCP), foundation types (Base gradation) and thickness, construction methods and material selection. And it will help MDOT find ways of identifying sections which are deteriorating at relatively rapid rates.

PCC Placement Time and Temperature on Transverse Cracking of JPCP's:

- High PCC placement temperature (>80 °F) during morning hours on hot summer days should be avoided for JPCP's as it causes increased transverse cracking. Nighttime paving would help reduce this problem, and may produce a smoother pavement. See attached paper by Hansen et al. Entitled, "Thermal Stress Development In Concrete Pavements At Early Ages", presented at the Sixth International Purdue Conference On Concrete Pavement Design And Materials For High Performance, November 18-21, 1997.

Moisture Related Effects On Pavement Distress Development:

- For OGDC pavements the literature suggests that enhanced pavement performance will result if the drainage system is maintained. For more detail see Appendix for Literature Review. This is consistent with the findings of this study that pavement sections suffering high amounts of distress, such as 77024A and 77023, also had evidence of poor drainage whereas pavements with good performance, such as 19042B and 19042C, had operating drainage systems.

6.0 REFERENCES

AASHTO (1993), "*Guide for Design of Pavement Structures*," American Association of State Highway and Transportation Officials, Washington, D. C.

ACPA (1995), "*Subgrades and Subbases for Concrete Pavements, Concrete Paving Technology*," TB011.02P, American Concrete Paving Association, Skokie, IL.

Army (1965), "*Drainage and Erosion Control, Subsurface Drainage Facilities for Airfield Pavements*," TM 5-820-2, Headquarters, Department of the Army, Washington, D. C.

ASTM (1995), "*1995 Annual Book of ASTM Standards*," Volume 04.02: Concrete and Aggregates, American Society for Testing and Materials, Philadelphia, PA.

Baldwin, J. S. (1987), "Use of Open-Graded, Free Draining Layers in Pavement Systems: A National Synthesis Report," Transportation Research Record 1121, Transportation Research Board, Washington, D. C., pp. 86-89.

Bunke, D. (1990), "Evaluation of Ohio Test Road for D-Cracking," Ohio Department of Transportation, Columbus, OH.

Byrum, C. R., and Hansen, W. (1994), "An Influence Function Approach to Analysis of Jointed Concrete Pavement," Transportation Research Record 1449, Transportation Research Board, Washington, D. C.

Carpenter, S. H. (1990), "*User's Manual and Technical Guide: DAMP Version 1.1 Drainage Analysis and Modeling Program*," FHWA-IP-90-012, Federal Highway Administration, Washington, D. C.

Cedergren, H. R. (1962), "Seepage Requirements of Filters and Pervious Bases," Paper 3363, ASCE, Volume 127.

Cedergren, H. R., Arman, J. A., and O'Brien, K. H. (1973). "Development of Guidelines for the Design of Subsurface Drainage for Highway Pavement Structural Sections," FHWA-RD-73-14, Federal Highway Administration, Washington, D. C.

Cedergren, H. R. (1987), "*Drainage of Highway and Airfield Pavements*," Robert E. Krieger Publishing Company, Malabar, FL., 289 pp.

Cedergren, H. R. (1994), "America's Pavements: World's Longest Bathtubs", Civil Engineering, Volume 64, No. 9, ASCE, New York, NY.

Cole, L. (1997), Presentation made at the Annual Meeting of the Transportation Research Board in Washington, D. C.

Crovetti, J. A., and Dempsey, B. J. (1991), "Pavement Subbases: Final Report," Project IHR-525, Report No. UILU-ENG-91-2005, Illinois Cooperative Highway Research Program, Illinois Department of Transportation, Springfield, IL.

Crovetti, J. A. (1995), "Analysis of Support Conditions Under Jointed Concrete Slabs Along USH 18/151: Final Report," Report No. WI/SPR-01-95, Wisconsin Department of Transportation, Madison, WI, March.

Crovetti, J. A. (1996), "Field Evaluation of Support Uniformity Under Joints Concrete Slabs," Accepted for Publication by the Transportation Research Board, Washington, D.C.

Darter, M. I. and Becker, J. M. (1984), "Concrete Pavement Evaluation Systems (COPES)," Vol. 1, Final Report, NCHRP, Transportation Research Board, Washington, D. C.

Dempsey, B. J., Carpenter, S. H., and Darter, M. I. (1982), "Improving Subdrainage and Shoulders of Existing Pavements-State of the Art." Report FHWA/RD-81/077, Federal Highway Administration, Washington, D. C.

Du, S., and Rummel, P. (1994), "Reconnaissance Studies of Moisture in the Subsurface with GPR," Institut fur Allgemeine und Angewandte Geophysic, Universitat Munchen.

ERES (1994), "*AASHTO Design Procedures for New Pavements: Participant's Manual*," FHWA -HI-94-023, National Highway Institute, Federal Highway Administration, U.S. Department of Transportation, Washington, D. C.

ERES (1996), "*NCHRP Project 134 Performance of Subsurface Pavement Drainage: An Interim Report*," Submitted to the National Cooperative Highway Research Program, Transportation Research Board, Washington, D. C.

FHWA (1990), "*Technical Guide Paper on Subsurface Pavement Drainage*," Technical Paper 90-01, Federal Highway Administration, Office of Engineering, Pavement Division, McLean, VA.

FHWA (1992), "*Drainable Pavement Systems —Participant's Notebook*," Demonstration Project 87, Publication No. FHWA-SA-92-008, Federal Highway Administration, 152 pp.

FHWA (1993), "*Techniques for Pavement Rehabilitation — A Training Course*," Fifth Addition, FHWA-HI-93-056, National Highway Institute, Washington, D. C.

FHWA (1994), "*AASHTO Design Procedures for New Pavements —Participant's Manual*," FHWA-HI-94-023, National Highway Institute, Washington, D. C.

Fleckstein, L. J., and Allen, D. L. (1996), "Evaluation of Pavement Edge Drains and Their Effect on Pavement Performance," Transportation Research Record 1519, Transportation Research Board, Washington, D. C.

Forsyth, R. A., Wells, G. K., and Woodstom, J. H. (1987), "Economic Impact of Pavement Subsurface Drainage," Transportation Research Record 1121, Transportation Research Board, Washington, D. C.

Forsyth, R. A. (1993), "Pavement Structural Design Practices," NCHRP Synthesis of Highway Practice 189, Transportation Research Board, Washington, D. C.

Freeman, R. B., and Anderton, G. L. (1994),"Unbound Drainable Base courses: Permeability Versus Unsurfaced Stability," *Infrastructure: New Materials and Methods of Repair* — Proceeding of the Third Materials Engineering Conference, ASCE, San Diego, CA., Nov. 13-16, pp. 685-692.

Grogan, W. P. (1994), "Evaluation of Drainable Base Courses for Pavements," *Infrastructure: New Materials and Methods of Repair* — Proceeding of the Third Materials Engineering Conference, ASCE, San Diego, CA., Nov. 13-16, pp. 693-700.

Gulden, W. (1974), "Investigation into the Causes of Pavement Faulting on the Georgia Interstate System," Georgia Department of Transportation.

Hagen, M. G., and Cochran, G. R. (1996), "Comparison of Pavement Drainage Systems," Transportation Research Record 1519, Transportation Research Board, Washington, D. C

Hall, M. J. (1995), "Cement-Stabilized Open-Graded Base Strength Testing and Field Performance Versus Cement Content," Transportation Research Record 1440, Transportation Research Board, Washington, D. C.

Hassan, H. F., White, T. D., McDaniel, R., and Andrewski, D. (1996), "Indiana Subdrainage Experience and Application," Transportation Research Record 1519, Transportation Research Board, Washington, D. C.

Heckel, L., (1997), "Performance Problems of Open Graded Drainage Layers Under Continuously reinforced Concrete Pavements in Illinois," Paper no. 970581. Presented at TRB Annual Meeting in Washington, D. C., 1997.

Hugenschmidt, J., Partl, M. N., de Witte, H., and Canton, U. (1996), "GPR Inspection of a Mountain Motorway - A Case Study," 6th International Conference on GPR, Sendai, Japan.

Janssen, D. J., Snyder, M. B., and Hansen, W. (1996), "Early and Long-Term Effects of Curling and Warping on Jointed Concrete Pavement," Interim Report, FHWA Project Number DTFH61-95-C-00021, Federal Highway Administration, Washington D. C.

Kazmierowski, A., et al. (1994), "Field Evaluation of Various Types of Open-Graded Drainage Layers," Transportation Research Record 1434, Transportation Research Board, Washington, D. C.

La Hue, S. P. (1990), National Advisory Committee — FHWA Demo Project #87 - Drainable Pavement Systems, Memo from the American Concrete Paving Association, Skokie, IL, May 7.

McAdam, J. L. (1820), "Report to the London Board of Agriculture."

Moss, G. M., Saak, A. W., Jennings, H. M., and Johnson, D. L., (1997), "Pooled Fund Study of Premature Concrete Pavement Deterioration," Draft Final Report, Department of Materials Science and Engineering, Northwestern University, Evanston, IL.

Moss, G. M., Saak, A. W., Jennings, H. M., and Johnson, D. L., (1997), "Pooled Fund Study of Premature Concrete Pavement Deterioration," Final Report, Region 7 Pooled Fund Study, Iowa DOT Research Project No. HR-1063, Northwestern University.

Moulton, L. K. (1980), "Highway Subdrainage Design," Report No. FHWA-TS-80-224, Federal Highway Administration.

Nettles, E. H., and Calhoun Jr., C. C. (1967), "Drainage Characteristics of Base Course Materials, Laboratory Investigation," Technical Report No. 3-786, U.S. Army Waterways Experimental Station, Vicksburg, MS.

Ray, M., and Christory, J. P. (1989), "Combating Concrete Pavement Slab Pumping: State of the Art and Recommendations," Proceedings from the Fourth International Conference on Concrete Pavement Design and Rehabilitation, Purdue University.

Rhodes, C. C. (1949), "Curing Concrete Pavements," Michigan State Highway Department, Project 42 B-14(2), Report 145.

Ridgeway, H. H. (1982). "Pavement Subsurface Drainage Systems." NCHRP Synthesis of Highway Practice 96, Transportation Research Board, Washington, D. C.

Smith, K. D., et al. (1990), "Performance of Jointed Concrete Pavements, Volume I — Evaluation of Concrete Pavement Performance and Design Features," Report FHWA-RD-89-136, Federal Highway Administration, Washington, D. C.

Smith, K. D., et al. (1995), "Performance of Concrete Pavements, Volume II — Evaluation of In-Service Concrete Pavements," Report FHWA-RD-95-110, Federal Highway Administration, Washington, D. C.

Teller, and Sutherland, E. C. (1935), "Observed Effects of Variations in Temperature and Moisture on the Size, Shape, and Stress Resistance of Concrete Pavement Slabs," Public Roads: Journal of Highway Research, USDA Volume 16, No. 9.

Topp, C. C., and Davis, J. L. (1982), "Measurement of Soil Water Content Using Time Domain Reflectometry," Associate Committee on Hydrology National Research Council of Canada, Fredericton, New Brunswick.

Van Wijk, A. J., et al. (1987), "Design to Prevent Pumping in Concrete Pavements," Unpublished Technical Summary, FHWA Contract No. DTFH61-82-C-00035, Federal Highway Administration, Washington, D. C.

Webster, S. L., Grau, R. H., and Williams, T. P. (1992), "Description and Application of Dual Mass Dynamic Cone Penetrometer," Final Report, Waterways Experiment Station, U.S. Army Corps of Engineer, Vicksburg, MS.

Wells, G. K. (1985), "Evaluation of Edge Drain Performance," FHWA/CA/TL-85/15, California Department of Transportation, Federal Highway Administration, Washington, D. C.

Wells, G. K. (1991), "California Experience with Permeable Bases and Retrofit Edge Drains," Western States Pavement Subdrainage Conference, Denver, CO.

Westergaard, H. M. (1926), "Stresses in Concrete Pavements Computed by Theoretical Analysis," Public Roads: Journal of Highway Research, USDA, Volume 7, No. 2.

THERMAL STRESS DEVELOPMENT IN CONCRETE PAVEMENTS AT EARLY AGES

Will Hansen, Associate Professor
Ashraf R. Mohamed, Research Fellow
Phil Mohr, Graduate Student
Department of Civil & Environmental Engineering
The University of Michigan

ABSTRACT

Internal stresses are present in Portland cement concrete pavement at early ages due to restrained curling and axial contraction. The risk of cracking in the pavement is largely associated with the temperature and tensile strength development of the concrete mixture as it cures. The temperature development is heavily influenced by heat released during cement hydration, the temperature of the concrete ingredients, and daily and seasonal fluctuations in ambient temperature. It has been observed that thermal stress development is most severe when the peak in the heat developed from hydration coincides with maximum daily ambient temperature. Thus, consideration should be given to placing concrete in the late afternoon or evening, especially during summer time placing conditions.

INTRODUCTION

It is well known that concrete undergoes dimensional changes as it cures due to temperature variations. As the hydration process commences, the developed heat causes the concrete to expand, while upon cooling the concrete contracts. In concrete pavements, as the slab is restrained externally by both its self-weight and subgrade friction, stresses will develop within the slab. A common practice is to install contraction joints to control the location of cracking. The amount of axial contraction that occurs is related to the heat developed in the concrete, the thermal expansion properties of the concrete constituents, the restraint from movement provided by foundation friction and adjoining slabs, and drying shrinkage. As the hydration takes place, heat is dissipated from the slab both to the foundation and to the air above. Because the ambient temperature fluctuates, and because heat is dissipated much more readily to the air than to the foundation, the temperature distribution through the slab thickness is not even. A temperature gradient develops which causes the slab to curl. For many years, the temperature gradient has been assumed to be linear (1,2,3). However, measurements of the temperature variation through the slab thickness reveal a highly non-linear distribution(4). Recently, a closed form solution has been developed by Mohamed and Hansen (5) for handling the non-linearity of the temperature profile. The contribution from both contraction and curling can induce significant stresses through the slab thickness, especially at early ages when concrete has not acquired its full tensile strength.

There exist many internal and external factors contributing to the early age (first few days after placement) temperature development. Internal factors include the heat generated from hydration of the cement and pozzolanic reactions, the thermal conduction properties of the concrete ingredients, and the slab dimensions (particularly its thickness). The external factors include changes in environmental factors such as the ambient air temperature and the underlying base temperature, solar radiation, wind velocity, and relative humidity (6,7). The heat exchange between the concrete and the environment occurs through conduction, convection and solar radiation.

The temperature of the concrete and the surroundings at the time at which the concrete is placed have a significant impact on the overall temperature development in the slab, and in turn on the resulting internal stresses. Furthermore, the time of day of placement will determine whether the peak in hydration coincides with, or counteracts the maximum daily temperature (8,9).

RESEARCH SIGNIFICANCE AND OBJECTIVE

Temperature variation within a concrete pavement slab at early ages has a significant influence on the slab's cracking tendency. Due to the restraint offered by the subgrade and the slab weight, internal stresses develop as a result of these variations. In some cases, especially at early ages, these stresses are comparable to the tensile strength of concrete. Controlling the temperature and time of concrete placing may result in a reduction in the cracking tendency of concrete pavement. Currently, pavement design does not explicitly account for thermal stresses. However, early cracking has been observed in concrete pavement slabs placed at high temperatures (>29.4 ^{O}C (85 ^{O}F)). For instance, a section of pavement on US-23 south of Dundee, Michigan was found to exhibit cracking within one month of opening to traffic. This roadway was placed on a windy 90^{O}F day. Cored samples from these slabs showed that these cracks were located within the top 5-7.5 cm (2-3 in) of the slab.

The objective of this investigation is to evaluate the internal thermal stresses that occur in a concrete pavement within the first few days after placing. The concrete mix design from US-23 is used, and various placing conditions are simulated.

RESEARCH APPROACH

The heat exchange between the concrete and its surroundings is a complex process. In this study a heat transfer analysis program ("Quadrel 1.5" (10)) is used for predicting the concrete temperature profile and maturity versus time for a variety of placement and environmental conditions. Solar radiation effects are not considered. The simulation process is based on a heat signature of the concrete mix, which has been identified through laboratory measurements using adiabatic calorimetry. The concrete strength (compressive and split tensile) development at early ages is measured in the laboratory. After predicting the temperature variation through the slab thickness at different time steps, the temperature gradient through the thickness is determined. As the temperature distribution has been found to be non-linear, the newly developed methodology (5) has been used to evaluate the stresses induced by such gradients. Strength development from the laboratory, adjusted for simulated conditions using the maturity function, are compared to these stresses to examine the risk of cracking.

PREDICTION OF TEMPERATURE PROFILES

In order to predict temperature profiles for a concrete pavement, a concrete batch with the same mix design is cast in the laboratory, from which adiabatic heat development is measured. Once this heat signature for the concrete has been obtained, field conditions such as slab thickness, temperature cycles, and wind speed are entered as input to a simulation program, which in turn develops the predicted temperature profile in the slab over time.

As this study utilizes commercially available software to simulate the temperature profiles, it is important to first verify whether the software is suitable for simulation of the conditions that are imposed in the study. This verification was done through a two stage procedure. First, the program was compared to known boundary cases. For example, to determine whether the program accurately measures the effects of temperature cycles, the slab thickness was reduced to near zero, which should cause the slab temperature to vary similarly to the air temperature. Indeed it was found that the program provides accurate results with respect to the cases investigated in this step.

Second, in order to determine the accuracy of the simulation program compared to measured data, a test slab section was cast in the laboratory. The slab was well insulated, and cast on an aggregate base to simulate similar conditions to those in the field. Thermocouples were placed through the thickness of the slab. Figure 1 shows the design and dimensions of the laboratory test slab. The slab was placed under controlled temperature and humidity conditions, and temperature measurements were recorded every 15 minutes for 3 days. The temperature was cycled over a 24 hour period from 15.6-26.7 ^{O}C (60 to 80 F) to simulate field conditions. Relative humidity was held constant at 50%. Concurrently, the adiabatic heat development for the same mix was measured as input to the computer simulation. Computer simulations were run on the same mix for the same conditions, and the results were compared. As can be seen from Figure 2, very close results have been found between the measured and simulated temperature variations. The small differences between the measured and predicted might be attributed not only to the fact that simulation does not account for all factors affecting heat transfer, but also to the imperfect boundary conditions in the experimental slab. Based on this finding, the computer simulation technique has been used for the remainder of the study.

Prediction of Thermal Stresses and Concrete Strength

The combination of the hydration and ambient temperatures lead to the early temperature rise in the concrete. It is somewhere near the peak temperature rise that final set occurs, and stresses can begin to develop in the slab. The formation of internal stresses in the slab follows through the mechanisms of uniform contraction and temperature curling. Figure 3 depicts the internal temperature loading in the concrete, which results in the development of stresses in the slab.

The uniform contraction of the slab is partially restrained by base course friction, as described by Okamoto (11). In this study, the restraint from movement is calculated from a modified form of the joint opening equation presented by Huang (12), and in essence accounts for the deformation the slab would undergo in space minus the amount the joint actually opens. When simplified, Equation 1 gives restrained portion of the movement due to uniform contraction.

$$\Delta L/L=(1-C)\alpha_t\Delta T/2 \qquad \text{[Eq. 1]}$$

in which ΔL is the restrained movement of the slab due to temperature change; L is the slab length; C is the adjustment factor due to slab-subbase friction; α_t is the coefficient of thermal expansion of the concrete taken as 1×10^{-5} /°C (5.5×10^{-6}/°F); and ΔT is the change in temperature. This determines the strain in the slab. Elastic modulus is calculated from strength using the ACI equation

$$E = 4.73\sqrt{f_c'}, \qquad \text{[Eq. 2]}$$

where E in GPa and f_c' in MPa ($E = 57,000\sqrt{f_c'}$ in psi units). The slab is assumed to behave in a linear elastic fashion, and stresses due to uniform contraction are calculated on that basis.

The second mechanism for stress development is the restrained curling in the slab. The slab tries to curl upward as the top cools more rapidly than the bottom. At the same time, the slab's weight restricts this movement. It has been documented (e.g. Thompson (4)) and will be shown that the temperature gradients are highly non-linear through the thickness of the slab. While traditional analysis of temperature gradient induced stress is based on linear gradient analysis, it has been shown (5) that this type of analysis may significantly underestimate the stress development through the thickness of the slab. For this reason, the recently developed closed form solution by Mohamed and Hansen (5) is being used in this context which takes into account the non-linear effects of temperature gradients through the slab thickness.

The concrete strength development begins at final set, and continues as the hydration reaction progresses. This process is highly influenced by curing conditions. The use of the maturity function concept allows the strength development under various field conditions to be related back to a standard laboratory condition. In this study, a laboratory batch was cast and tested to develop the standard maturity condition for the field mix design. The maturity function is then used to relate the laboratory strength development to the various batch temperatures and placing times in question.

REFERENCE CASE: US-23 MICHIGAN

In order to investigate the effect of time and temperature of placement on the cracking tendency of concrete pavement, a reference case is needed. The reference case in this study is a section of pavement on US-23 south of Dundee, Michigan. It has been found to exhibit cracking within one month of opening to traffic. This roadway was placed on a windy 32 °C (90 °F) day. Thus, all parameters in this study are limited to the conditions that existed in this case. For instance, the temperature has been varied between 21-35 °C (70-95 °F), which represents a typical temperature variation in that location. Furthermore, the friction coefficient C in Eq. (1) has been set to 0.8, resembling that recorded for the type of base course in the reference study. The slab dimensions are 3.66x8.25 m(12x27 ft).

Simulation of Placing Conditions for the Reference Case

Once it has been established that the simulation software provides acceptable results, the conditions in the field at US-23 can be simulated to determine the cracking susceptibility of the pavement during the first few days after placement. This field condition will be referred to as case 1, and is shown in Table 1. For this and all placing conditions studied, a 26.7 cm (10.5 in.) slab thickness and 12.5 km/h (7.5 mph) wind speed were used.

As shown in Figure 4, the temperature at the top of the slab is typically cooler than at the bottom at early ages, and the gradients are highly nonlinear. This causes the pavement to curl upward. The upward curling of the slab is restrained by its own weight. Therefore, the concrete develops tensile stresses at the top. Stresses due to nonlinear temperature gradients are calculated based on the methodology in (5). The stresses due to curling account for the majority of stresses developed within the first 24 hours. The distribution of stresses through the slab thickness over time is shown in Figure 5.

As shown in Figure 6, the average temperature of the concrete rises to roughly 43.3 ^{o}C (110^{o}F) and then drops to less than 29.4 ^{o}C (85^{o}F) over the next 2 days. This 13.9 ^{o}C (25^{o}F) drop over such a short period of time causes the slab to contract very rapidly. The frictional restraint from the base does not allow the concrete to contract fully, causing it to develop tensile stresses at the mid span.

Due to thermal effects alone, the tensile stresses that develop in the concrete amount to approximately 1.378 MPa (200 psi) 24 hours after placement. This is approaching the tensile strength which is only about 2.067 MPa (300 psi) at 24 hours after placement. For this study, moisture shrinkage is not taken into account. If the stresses developed due to moisture loss are added, the tensile stresses in the concrete would most likely exceed the tensile strength and cause the concrete to crack at the top near the mid span of the slab.

Effects of Varying Batch Temperature and Placing Time on Risk of Early Cracking

In addition to the US-23 field condition, the effects of varying time of placement and concrete temperature at placement are also investigated. Seen in Table 1 are the conditions of all test cases that are studied.

It can be seen from Figures 7-9 that the development of stress in the slab is significantly influenced by both time of placement and concrete temperature at time of placement. This is particularly evident for the afternoon and evening cases, where stress development is delayed because of the offset between hydration and ambient temperatures. The influence of reduced placing temperature has the greatest effect on uniform contraction of the slab. Internal stress development due to nonlinear gradients is not significantly influenced by changes in batch temperature at placement. A combination of low batch temperature and late in the day placement can avoid significant stress development until later ages, when the concrete has gained considerably more strength. By controlling the temperature rise, the risk of cracking due to thermal stresses can be reduced significantly.

CONCLUSIONS

- The thermal stresses that develop in concrete pavements placed during high temperatures (>29.4 ^{o}C (85 ^{o}F)) are significant within the first several days after placement.
- Delaying concrete placement until the afternoon or evening can delay the buildup of thermal stresses in the slab until the concrete has gained considerably more strength.
- Reducing batch temperature has a limited effect in reducing internal stresses, but is accompanied by a corresponding reduction in tensile strength gain at early ages.
- The retardation of stress development in afternoon placements is caused by the peak temperature from hydration being reached during the coolest period of the day, reducing the overall temperature rise in the concrete.
- More work is needed to explore the other factors affecting the cracking tendency of concrete at early ages. This includes, but is not limited to, the range of temperature variation, the slab thickness, and the concrete thermal properties, as well as inclusion of radiation effects.

Table 1. Placing conditions of the various test cases.

	Case 1	Case 2	Case 3	Case 4	Case 5	Case 6	Case 7
Air Temp.	21-35	21-35	21-35	21-35	21-35	21-35	21-35
Batch Temp. at Placement	32.2	23.9	15.6	32.2	15.6	26.7	15.6
Soil Temp.	26.7	26.7	26.7	26.7	26.7	21.1	21.1
Time of Placement	8 AM	8 AM	8 AM	4 PM	4 PM	8 PM	8 PM

$1^{o}F=(f-32)/1.8 \quad {}^{o}C$

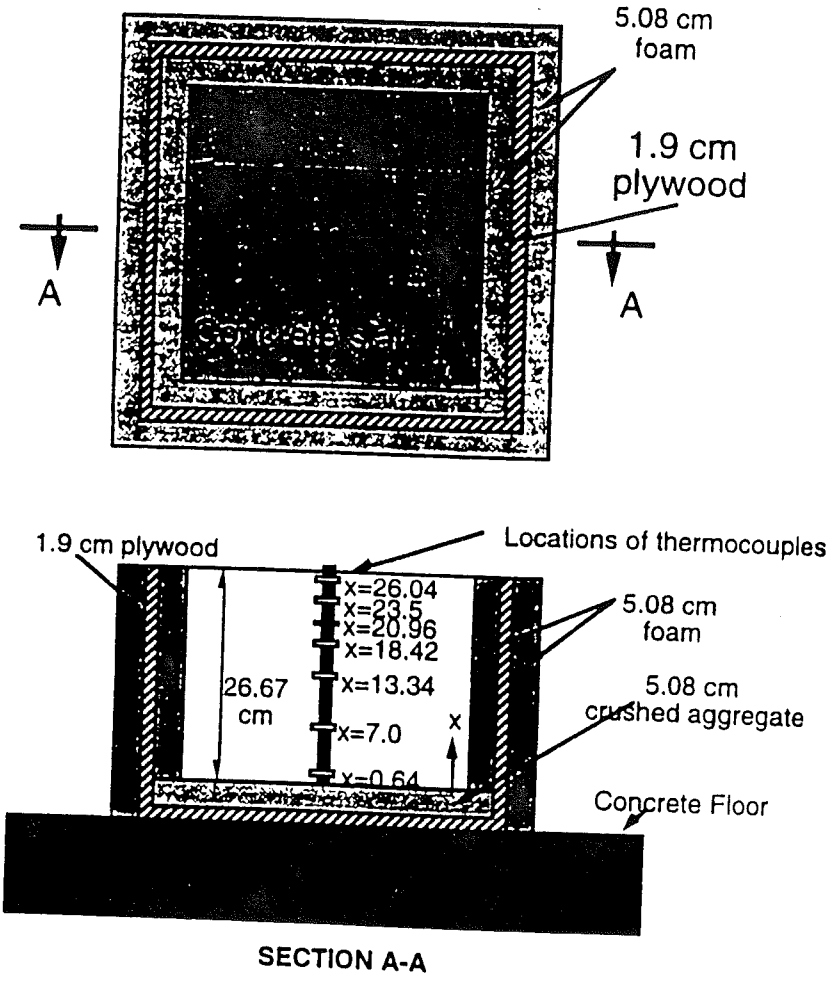

Figure 1.

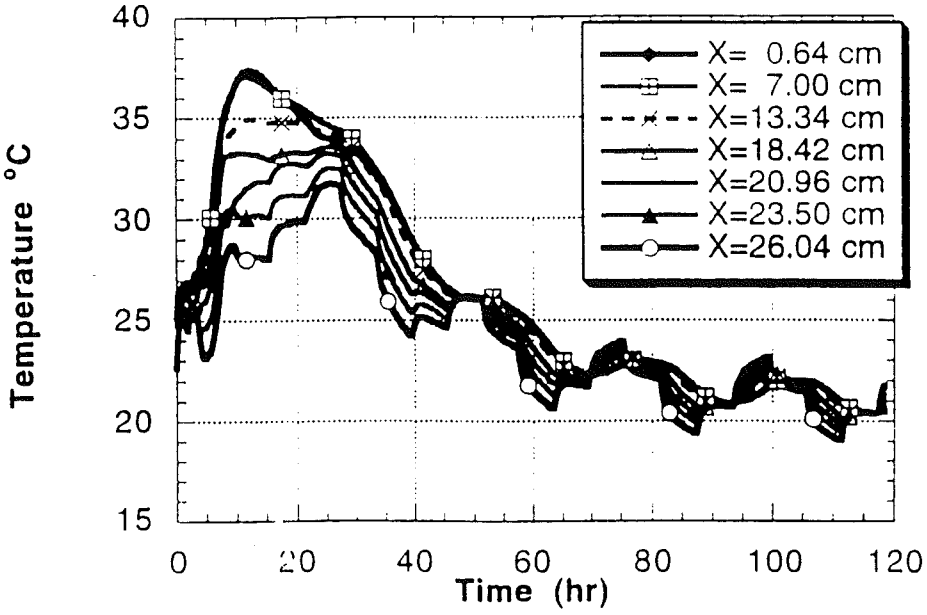
Temperature °C
40
35
30
25
20
15
0
20
40
60
80
100
120
Time (hr)
X= 0.64 cm
X= 7.00 cm
X=13.34 cm
X=18.42 cm
X=20.96 cm
X=23.50 cm
X=26.04 cm

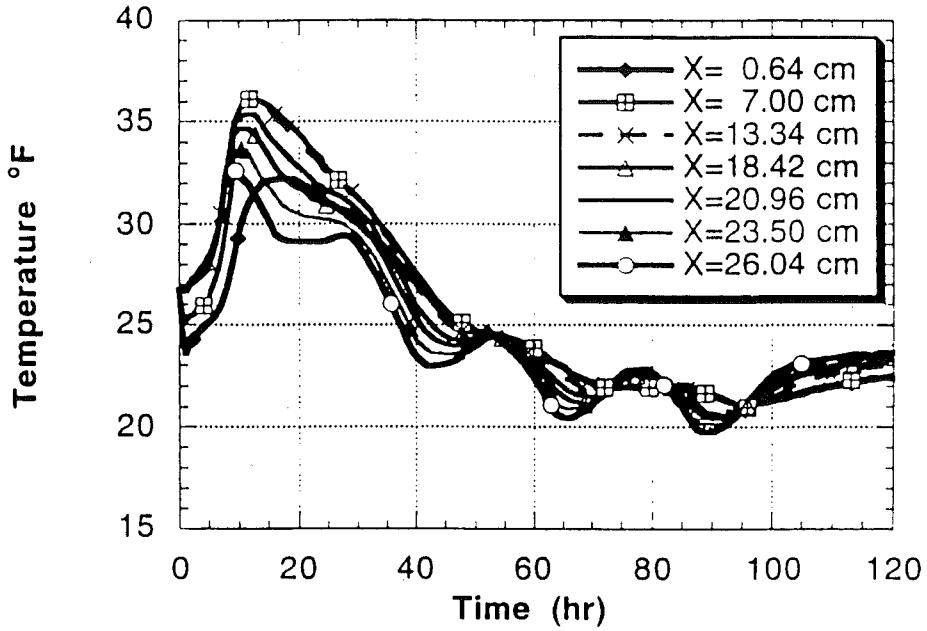
Temperature °F
40
35
30
25
20
15
0
20
40
60
80
100
120
Time (hr)
X= 0.64 cm
X= 7.00 cm
X=13.34 cm
X=18.42 cm
X=20.96 cm
X=23.50 cm
X=26.04 cm

Figure 2.

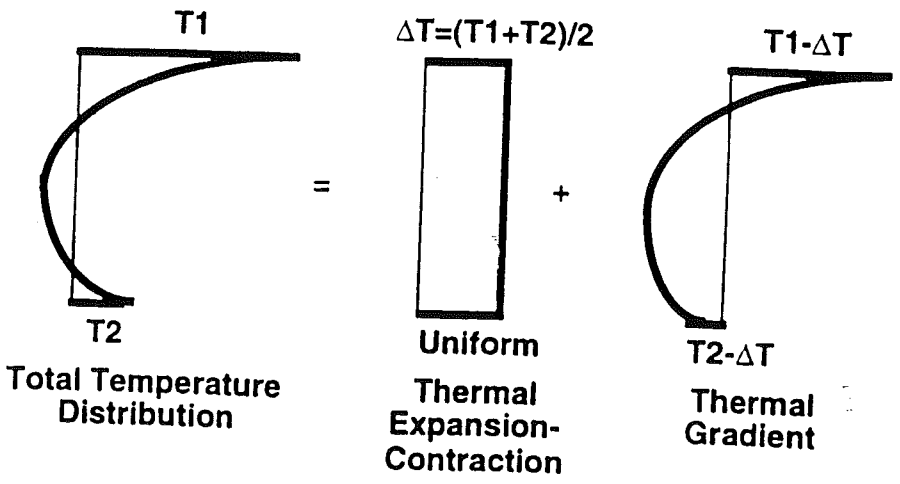

Figure 3.

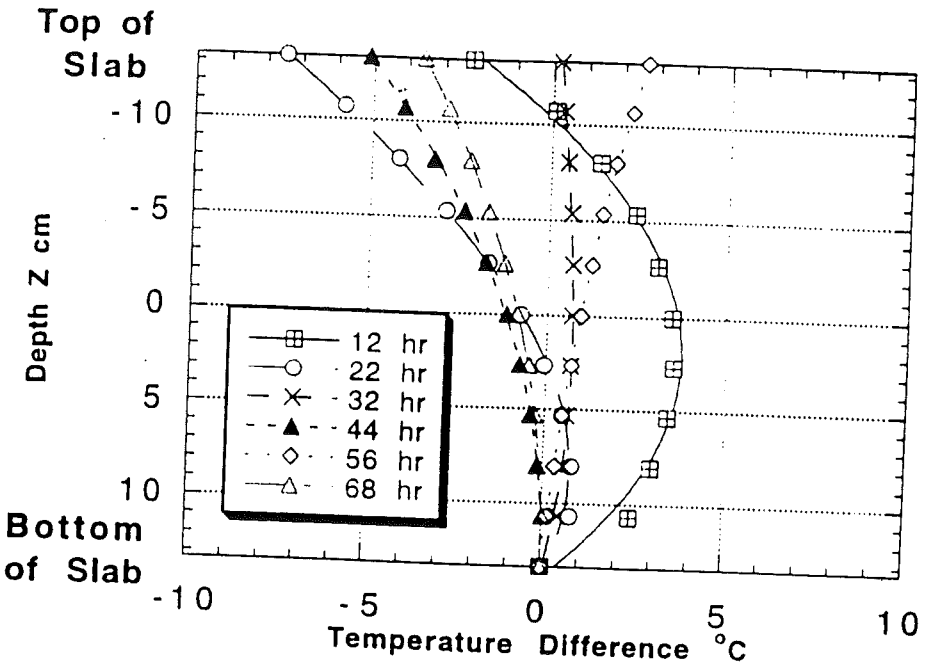

Figure 4.

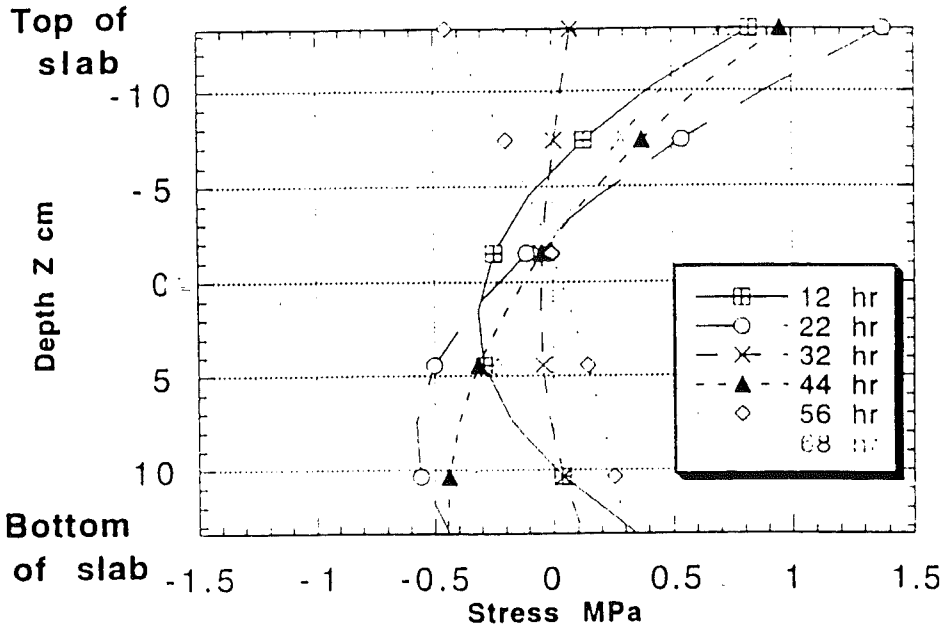

Figure 5.

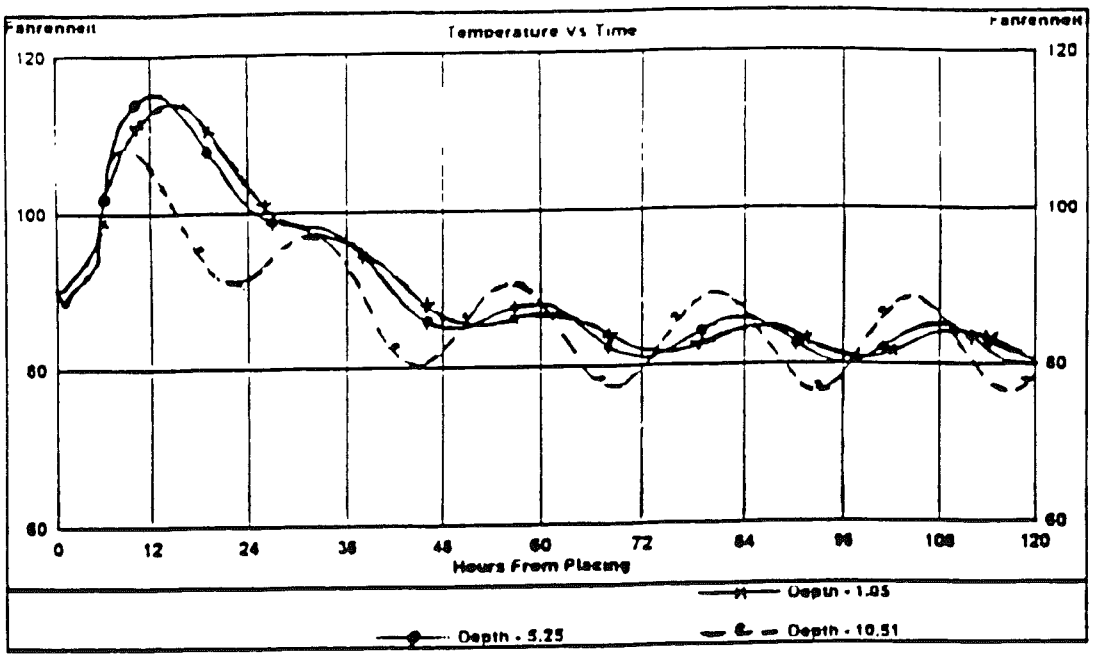

Figure 6.

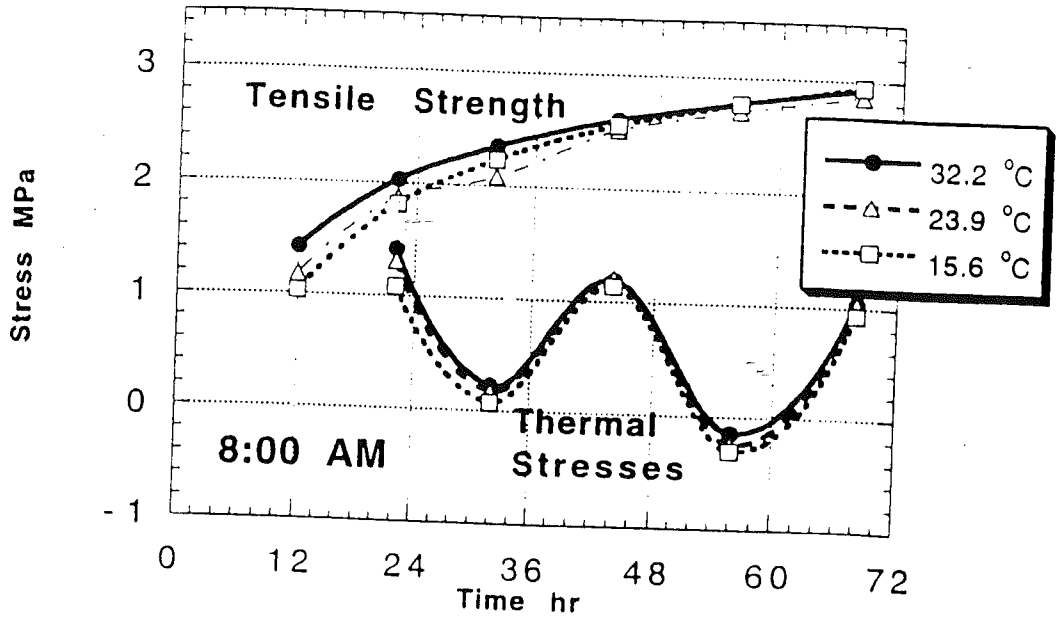

Figure 7.

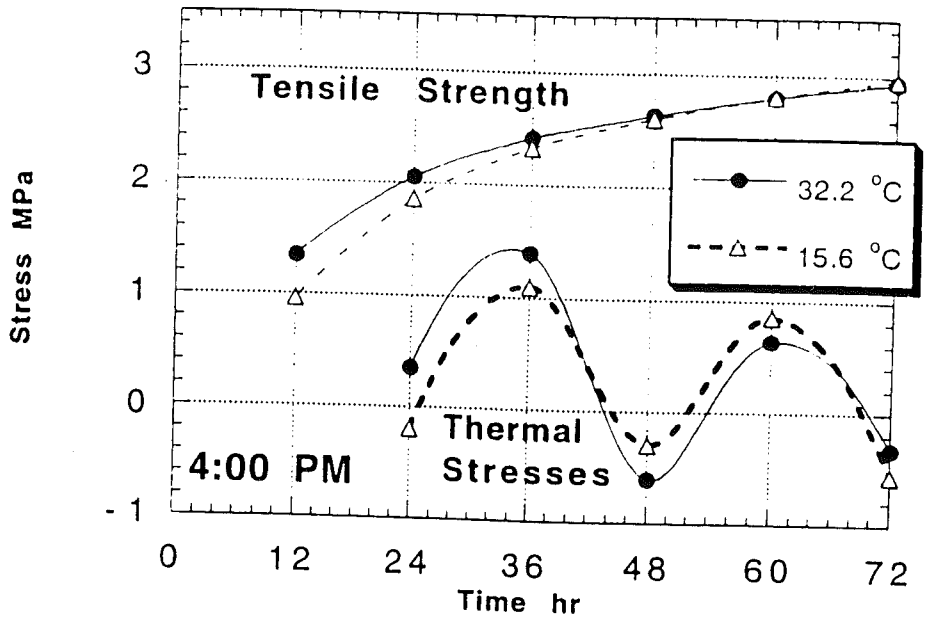

Figure 8.

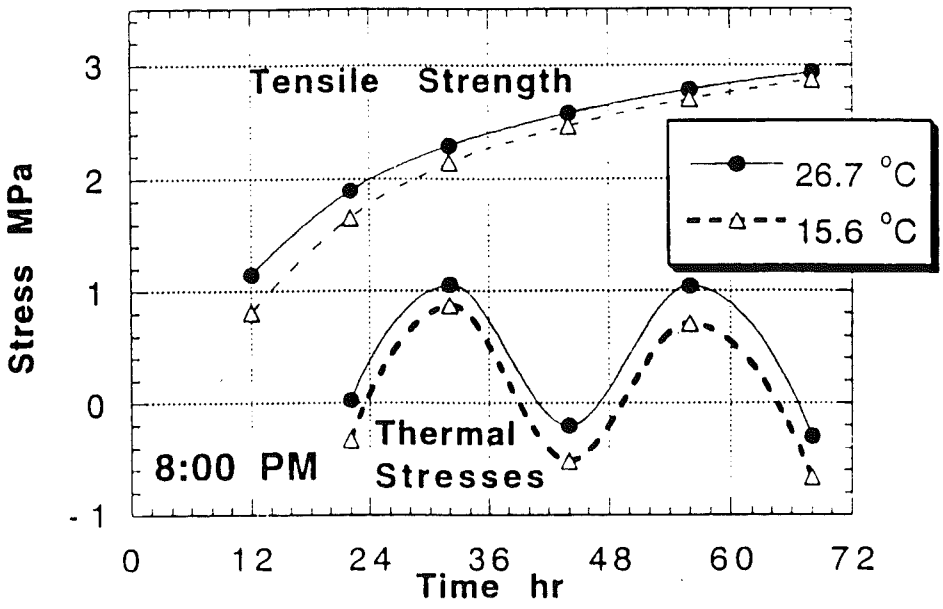
Tensile Strength
26.7 °C
15.6 °C
Thermal Stresses
8:00 PM
Stress MPa
Time hr
3
2
1
0
- 1
0
12
24
36
48
60
72

Figure 9.

REFERENCES

1. Westergaard, H. M., Computation of Stresses in Concrete Roads. In Proc. of the Fifth Annual Meeting, Vol. 5, Part 1, Highway Research Board, 1926, pp. 90-112.

2. Westergaard, H. M., New Formulas for Stresses in Concrete Pavements of Airfields. American Society of Civil Engineers, Transactions, Vol. 113, 1947, pp. 425-444.

3. Bradbury, R. D., Reinforced Concrete Pavements. Wire Reinforcement Institute, Washington D.C., 1947.

4. Thompson, M. R., Dempsey, B. J., Hill, H., and Vogel, J. Characterizing Temperature Effects for Pavement Analysis and Design. In Transportation Research Record 1121, TRB, National Research Council, Washington D.C., 1987, pp. 14-22.

5. Mohamed, A. R. and Hansen, W. Prediction of Stresses in Concrete Pavement Subjected to Non-Linear Gradients. Journal of Cement and Concrete Composites, Vol. 18, 1996, pp. 381-387.

6. Tritsch, S. Temperature Management of Slabs. Chapter 5 of "Accelerated Paving Techniques-State-Of-The-Art Report", Special Project 201, USDOT, FHWA, 1994.

7. Springenschmid, R. (ed.). Thermal Cracking in Concrete at Early Ages. Proceedings of the International RILEM Symposium, vol. 25, E & FN Spon, Chapman & Hall, London, 1994.

8. Andersen, P., Andersen, M., and Whiting, D. A Guide to Evaluating Thermal Effects in Concrete Pavements. Strategic Highway Research Program (SHRP), National Research Council, Washington, D.C., 1992.

9. McCullough, F. and Suh, Y., Effect of the Cement Hydration and Placement Time on the Early-Age Cracking of CRCP. Transportation Research Board, Washington, D.C., 1994.

10. "Quadrel 1.5" Digital Site Systems, Inc., Pittsburgh, PA 1994.

11. Okamoto, P., Nussbaum, P., Smith, K., Darter, M., Wilson, T., Wu, C., and Tayabji, S. Guidelines for Timing Contraction Joint Sawing and Earliest Loading for Concrete Pavements. FHWA-RD-91-079, Washington, D.C., Federal Highway Administration, 1994.

12. Huang, Y. Pavement Analysis and Design. Prentice Hall, Englewood Cliffs, New Jersey, 1993.

ACKNOWLEDGMENTS

The authors wish to acknowledge the support for this study from the National Science Foundation Center for Advanced Cement-Based Materials (ACBM). The authors also wish to thank the Michigan Department of Transportation (MDOT) for its keen interest and gracious cooperation in this project.